Montclair State University

MONTCLAIR STATE UNIVERSITY

Montclair State University Digital Commons

Department of Earth and Environmental Studies Faculty Scholarship and Creative Works

Department of Earth and Environmental Studies

2019

Environmental Forensic Characterization of Former Rail Yard Soils Located Adjacent to the Statue of Liberty in the New York/New Jersey Harbor

Diane Hagmann
Montclair State University

Michael A. Kruge
krugem@mail.montclair.edu

Matthew Chi-Hymn Cheung
Montclair State University

Maria Mastalerz
Indiana University - Bloomington

José Luis Gallego
University of Oviedo

See next page for additional authors

Follow this and additional works at: https://digitalcommons.montclair.edu/earth-environ-studies-facpubs



Part of the Analytical Chemistry Commons, Environmental Chemistry Commons, Environmental Monitoring Commons, and the Soil Science Commons

MSU Digital Commons Citation

Hagmann, Diane; Kruge, Michael A.; Cheung, Matthew Chi-Hymn; Mastalerz, Maria; Gallego, José Luis; Singh, Jay Prakash; Krumins, Jennifer; Li, Xiaona N.; and Goodey, Nina M., "Environmental Forensic Characterization of Former Rail Yard Soils Located Adjacent to the Statue of Liberty in the New York/New Jersey Harbor" (2019). *Department of Earth and Environmental Studies Faculty Scholarship and Creative Works*. 63.
https://digitalcommons.montclair.edu/earth-environ-studies-facpubs/63

This Article is brought to you for free and open access by the Department of Earth and Environmental Studies at Montclair State University Digital Commons. It has been accepted for inclusion in Department of Earth and Environmental Studies Faculty Scholarship and Creative Works by an authorized administrator of Montclair State University Digital Commons. For more information, please contact digitalcommons@montclair.edu.

Authors

Diane Hagmann, Michael A. Kruge, Matthew Chi-Hymn Cheung, Maria Mastalerz, José Luis Gallego, Jay Prakash Singh, Jennifer Krumins, Xiaona N. Li, and Nina M. Goodey

This article is available at Montclair State University Digital Commons: https://digitalcommons.montclair.edu/earth-environ-studies-facpubs/63

Preprint: Hagmann D.F., Kruge M.A., Cheung M., Mastalerz M., Gallego J.L.R., Singh J.P., Krumins J.A., Li X., Goodey N. (2019) Environmental forensic characterization of former rail yard soils located adjacent to the Statue of Liberty in the New York/New Jersey harbor. *Science of the Total Environment* **690**:1019-1034. https://doi.org/10.1016/j.scitotenv.2019.06.495

Environmental forensic characterization of former rail yard soils located adjacent to the Statue of Liberty in the New York/New Jersey harbor

Diane F. Hagman[1]
Michael A. Kruge*[1]
Matthew Cheung[2]
Maria Mastalerz[3]
José L.R. Gallego[4]
Jay P. Singh[1]
Jennifer Adams Krumins[2]
Xiaona N. Li[1]
Nina M. Goodey*[5]

[1]Department of Earth and Environmental Science, Montclair State University, Montclair, NJ, USA.
[2]Department of Biology, Montclair State University, Montclair, NJ, USA.
[3]Indiana University, Bloomington, Indiana, USA
[4]University of Oviedo, Mieres, Asturias, Spain
[5]Department of Chemistry and Biochemistry, Montclair State University, Montclair, NJ, USA.
*Co-Corresponding Authors: Nina M. Goodey, email: goodeyn@mail.montclair.edu, ph: 973-666-1368 and Michael A. Kruge, email: krugem@mail.montclair.edu

Highlights

- We characterized organic and inorganic substances at a major urban brownfield site
- We detected abundant petroleum- and coal-derived biomarkers and PAHs in the soil
- Both barren low-functioning and forested soils contained similar organic compounds
- The barren site featured very high heavy metal loads and dormant microbial life
- Chemical and ecological studies are critical to brownfield restoration efforts

Graphical Abstract



Abstract

Identifying inorganic and organic soil contaminants in urban brownfields can give insights into the adverse effects of industrial activities on soil function, ecological health, and environmental quality. Liberty State Park in Jersey City (N.J., USA) once supported a major rail yard that had dock facilities for both cargo and passenger service; it was later closed off to the public, and a forest developed and spread in the area. The objectives of this study were to: 1) characterize the organic and inorganic compounds in Liberty State Park soils and compare the findings to an uncontaminated reference site (Hutcheson Memorial Forest); and 2) identify differences between the barren low-functioning areas and the forested high-functioning areas of the brownfield. Soil samples were solvent-extracted, fractionated, and analyzed by gas chromatography-mass spectrometry and subjected to loss-on-ignition, pyrolysis-gas chromatography-mass spectrometry, inductively-coupled-plasma mass spectrometry, and optical microscopy analyses. Compared to soil from the reference site, the forested soils in Liberty State Park contained elevated percentages of organic matter (30–45 %) and more contaminants, such as fossil-fuel-derived hydrocarbons and coal particles. Microscopy revealed bituminous and anthracite coal, coke, tar/pitch, and ash particles. Barren and low-functioning site 25R had a similar organic contaminant profile but contained a higher metal load than other Liberty State Park sites and also lacked higher plant indicators. These can obscure the signatures of contaminants, and data from adjacent barren and vegetated sites are valuable references for soils studies. A deeper understanding of the chemistry, biochemistry, and ecology of barren soils can be leveraged to prevent land degradation and to restore dysfunctional and phytotoxic soils.

Keywords: Brownfield, heavy metals, polycyclic aromatic hydrocarbons, soil forensics, pyrolysis-GC-MS, petrography, industrial barrens

1. Introduction

Past industries have altered ecosystems by introducing inorganic and organic contaminants into soils (Alker et al., 2000; Gallego et al., 2016; Qian et al., 2017; Thornton et al., 2008). Specifically, former rail yard soils remain contaminated years after operations have ceased (Jackson, 1997). Loading, unloading, and the train engines themselves can introduce both inorganic compounds such as heavy metals and organic contaminants including polycyclic aromatic hydrocarbons (PAHs) into the soil (Jackson, 1997; Lacey and Cole, 2003; Liu et al., 2008; Malawska and Wilkomirski, 1999; Malawska and Wiłkomirski, 2000; Malawska and Wiołkomirski, 2001; Wiłkomirski et al., 2011). Organic contaminants can originate from lubricating oils, coal, oil, fertilizers and herbicides (Biache et al., 2017; Wiłkomirski et al., 2011). PAHs, many of which are toxic or mutagenic to humans, plants, and animals, (Brooks, 2004; Smith et al., 2006) can originate from incomplete combustion of coal (Haritash and Kaushik, 2009).

Liberty State Park (LSP) in Jersey City, New Jersey is located across the Hudson River from lower Manhattan and the Statue of Liberty and once supported a rail yard (Fig. 1A). Originally, LSP consisted of mudflats and salt marsh but was later filled in with New York City construction debris and municipal waste to prepare for the construction of the Central Railroad of New Jersey. The railroad was built between 1860 and 1919, operated until 1967, and was closed in 1970 (Gallagher et al., 2008a). Part of LSP was remediated but a 100-ha un-remediated site, our study area, was fenced to restrict public access. Despite its history of contamination, most

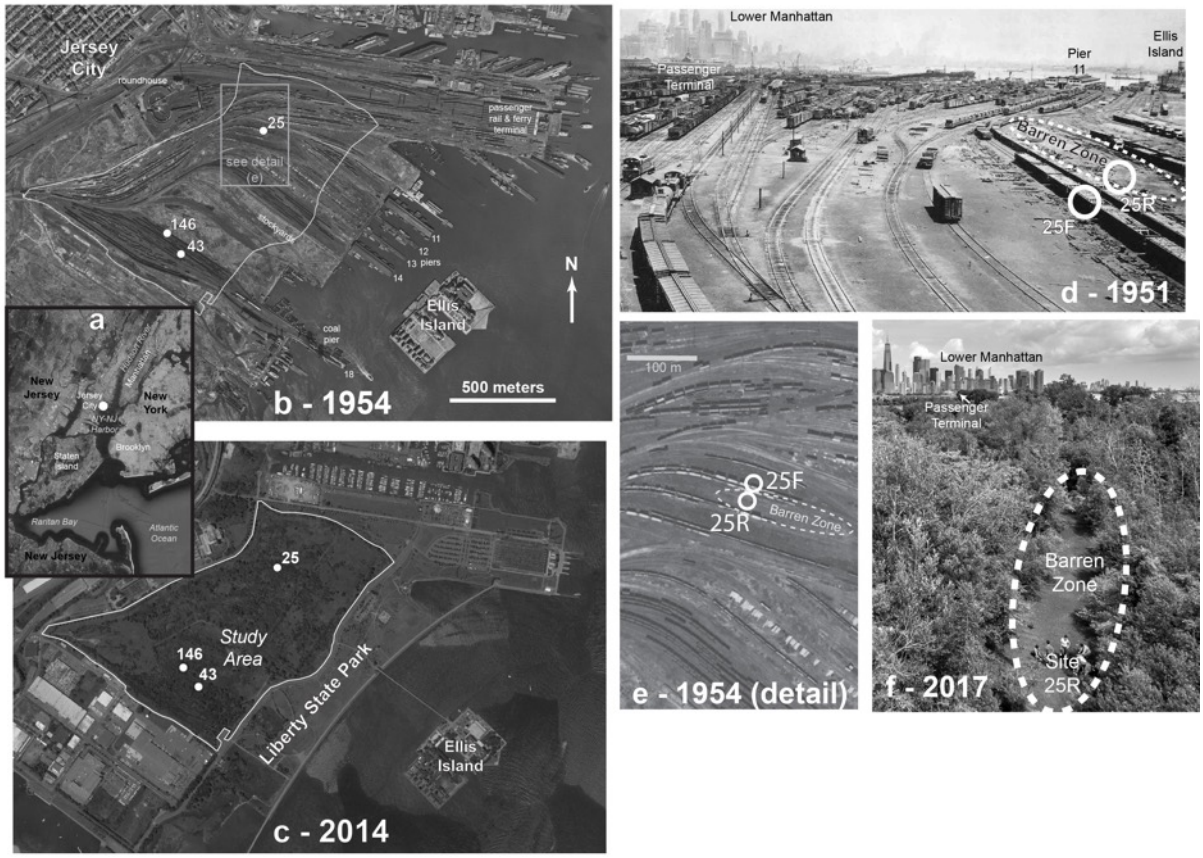
areas within our un-remediated study site support a biodiverse and productive forest (Gallagher et al., 2008a). Figure 1C shows the locations of our sites within the study area (43, 146, and 25). The organic compounds at LSP had not been previously analysed but coal fragments are visible throughout the site.

We previously discovered high enzyme activities at LSP site 146, which has high heavy metal loads (Hagmann et al., 2015). This finding was surprising because heavy metal and organic contaminants are often thought to decrease soil microbial functioning (Alisi et al., 2009; Buettner and Valentine, 2011; Hamdi et al., 2007; Sprocati et al., 2012). Because organic contaminants can play a role in soil functioning (Baran et al., 2004; Shen et al., 2005) and display additive effects in combination with heavy metals (Maliszewska-Kordybach and Smreczak, 2003; Shen et al., 2005), we identified organic contaminants at different sites within LSP that might lead to differences in enzymatic activities. It is important to study both inorganic and organic compounds to understand historic industrial activities (Ortiz et al., 2016a).

Figure 1

The use of pyrolysis gas chromatography – mass spectrometry (Py-GC-MS) is only beginning to see wide application in characterization of brownfield contaminants (Kruge, 2015; Kruge et al., 2018; Lara-Gonzalo et al., 2015). Here we studied LSP soils via Py-GC-MS and GC-MS combined with organic petrography and determination of soil enzyme activities, major and trace elements, total organic matter, and microbial counts. This unique combination of methods, including the concurrent identification of organic and inorganic pollution with measurements of enzymatic function and microbial counts, provides a multidimensional understanding of the contaminants in LSP soils.

Fig. 1. Liberty State Park is located in Jersey City, New Jersey (a). Aerial images from: U. S. Geological Survey: 1954 (b, e) and 2014 (c). Study sites within LSP are indicated on the map (43, 146, 25F, 25R). A historical photograph of 25F and 25R from 1951 (d). Sites 25F and 25R are located next to each other; 25R is in a strip of land without vegetation (f). Photo Credits: d: Andrew Bologovsky f: Mike Peters Montclair State University. Photos used with permission.



Sites were chosen in LSP and at the reference site at Hutcheson Memorial Forest (HMF) that would allow us to answer questions about the impact of industrial activities and vegetation on organic contaminant profiles in the soils. Soils were characterized at four sites (43, 146, 25F, and 25R) within the un-remediated and closed-off LSP area. Our first hypothesis was that there will be more fossil fuel biomarkers at LSP compared to HMF. According to historic photographs shown in Figure 1B, sites 43 and 146 lie along tracks to a coal pier while sites 25F and 25R are located next to each other and along the route to "Pier 11" (Fig. 1D). All LSP sites have a history of industrial contamination while the reference site HMF does not. Site 25R lacks plants while the other three LSP sites (43, 146, and 25F) and reference site are vegetated. Our second hypothesis was that the barren site 25R will have more or different contaminants compared to the forested sites at LSP. Our two primary objectives were to: 1.) characterize the organic and inorganic compounds at LSP and compare the findings to a reference site HMF; and 2.) identify differences between the barren site 25R (area with no vegetation) and forested areas at LSP.

2. Methods

2.1 Site description

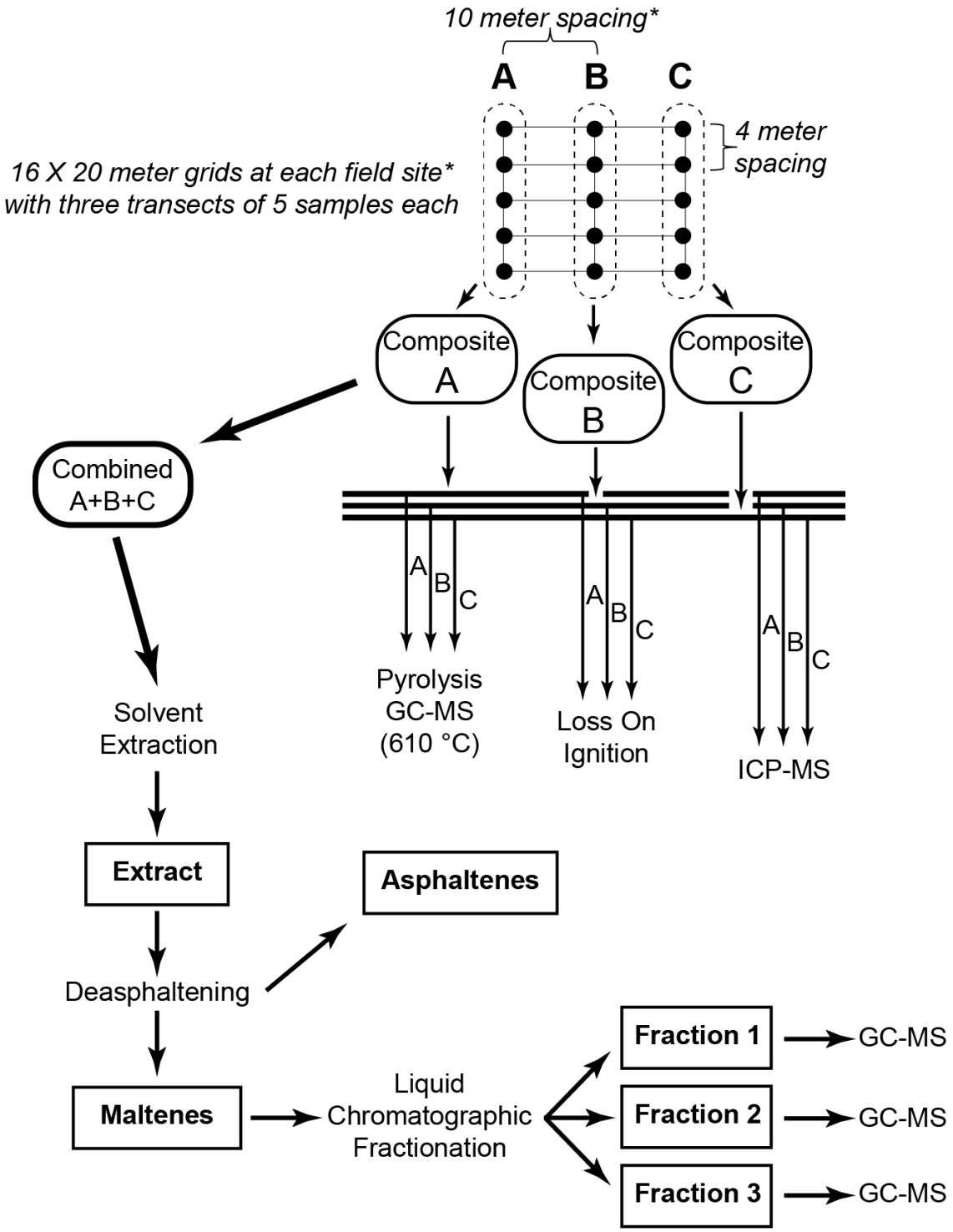
Soil samples were collected from four sites located within an un-remediated, restricted-access, 100-ha plot within LSP, Jersey City, NJ, USA (40° 42" 16 N, 74° 03' 06 W, Fig. 1A, B). LSP was formerly a major rail yard and dock facility built on estuarine marshland and was abandoned around 1969 (Gallagher et al., 2008a). In the intervening decades, dense forest cover took over the restricted access plot without human intervention.

Soils for this study were collected from three different vegetated sites within LSP, including 43, 146, and 25F (Fig. 1C). A fourth site—25R that is adjacent to 25F—is on a strip of

91 land that remains anomalously barren (Fig. 1F). As a reference, soil was also collected from a
92 location within HMF in Franklin Township, N.J—an abandoned agricultural field with no history
93 of industrial use or contamination about 60 km southwest of LSP—having the same natural
94 successional timeframe.
95
96 2.2 Soil collection and preparation
97 Soil was collected in July 2016 from LSP sites 25F, 25R, 43, and 146 as well as the reference
98 site HMF. For this study, five samples were collected along a transect at intervals of 4 m for this
99 study into separate bags (depth of 10 cm below the leaf-litter). The samples were stored in a
100 refrigerator (4 °C). At the lab the soils were sieved through a 2-mm sieve and equal amounts of
101 the five samples along a transect were combined into one bag labelled with the transect name and
102 site (e.g., 43A). At each site, five samples were collected along three parallel transects 10 m
103 apart. Thus, fifteen soil subsamples from a 16 by 20 m field grid were combined into three
104 composite samples (one for each transect), as seen in Figure 2. For each site, the three
105 composites samples were submitted separately for laboratory analysis. Figure 2 shows an
106 overview of the experimental procedures we used to determine the organic composition of the
107 soils as described in sections 2.4 and 2.5.
108
109 2.3 Percent organic matter
110 The percent organic matter was determined by loss on ignition (LOI). This procedure is
111 described in Hagmann et al. 2015. Briefly, soil was dried at 70°C for 24 hours. The soil was
112 ground using a mortar and pestle and samples were heated to 550°C for 4 hours. The percent

113 organic matter was determined gravimetrically. Results are presented as the mean values of the
114 three composite soil samples taken at each site.
115
116 2.4 Extraction, LC fractionation and GC-MS
117 For each site, only one analysis was performed, on a global sample combining each of the three
118 transect composites (Section 2.2) in equal measure. Dry soil samples < 2 mm (7.8 – 11.0 g_{dry})
119 underwent solvent extraction as described in Lara-Gonzalo et al. 2015. Briefly, soils were
120 extracted using dichloromethane:methanol (3:1, v/v) in a Soxtherm system (Gerhardt analytical
121 systems: Königswinter, Germany). The extract was concentrated by rotary evaporation. Aliquots
122 of the Soxtherm extract were fractionated and gravimetrically quantified by open column liquid
123 chromatography (LC). First, maltenes and asphaltenes were separated by filtering through 0.45
124 μm filters using hexane and dichloromethane, respectively; then, maltenes were fractionated into
125 three fractions by LC in columns filled with silica gel and alumina. Fraction 1 (predominantly
126 aliphatic hydrocarbons) was eluted with hexane, Fraction 2 (predominantly aromatic
127 hydrocarbons) with a mix of dichloromethane:hexane (7:3, v/v) and finally, Fraction 3
128 (predominantly polar compounds) with dichloromethane:methanol (1:1, v/v).
129 Figure 2
130 The analysis of the LC fractions was carried out by GC/MS. The injection of the extracts was
131 performed on a GC/MS QP-2010 Plus (Shimadzu: Kyoto, Japan). A capillary column DB-5ms
132 (5% phenyl 95% dimethylpolysiloxane; 60 m × 0.25 mm i.d. × 0.25 μm film) from Agilent
133 Technologies was used with helium as carried gas at 1 mL/min. The initial oven temperature was
134 50 ºC (held for 2 min) and ramped at 2.5 ºC min^{-1} up to 310 ºC and held for 45 min. The mass
135 spectrometer was operated in electron ionization mode (EI) at 70 eV. It was calibrated daily by

Fig. 2. Flow chart illustrating the experimental design for the experiment.



136 autotuning with perfluorotributylamine (PFTBA) and the chromatograms were acquired in full-
137 scan mode (mass range acquisition was performed from 45 to 500 m/z). Compounds were
138 identified using the NIST 2014 Mass Spectral Library (NIST 2014/EPA/NIH) and by reference
139 to the literature.
140
141 2.5 Pyrolysis-Gas Chromatography-Mass Spectrometry (Py-GC-MS)
142 For samples HMF, LSP 43, and LSP 146, Py-GC-MS was performed using a CDS Analytical
143 5000 Pyroprobe (Oxford, Pennsylvania, USA) coupled to a Thermo Electron DSQ GC/MS
144 (Madison, Wisconsin, USA) equipped with an Agilent DB-1MS column (30 m × 0.25 mm i.d. ×
145 0.25 μm film thickness). The GC oven temperature was programmed from 50 °C to 300 °C (at 5
146 °C min^{-1}), with an initial hold of 5 min at 50 °C and a final hold of 15 min at 300 °C. Pyrolysis
147 was performed for 20 s at 610 °C. The MS was operated in full scan mode (50-500 Da, 1.08
148 scans s^{-1}). Quality control was performed by separately analyzing the three composited samples
149 from each site (Section 2.2). For each site, the three yielded very similar results; therefore, only
150 one was used to represent the site in this paper. Compounds were identified using the NIST MS
151 library and by reference to the literature.
152
153 2.6 Organic petrography
154 For petrographic analysis, soil samples were mixed with Lucite powder and prepared into pellets
155 in a Leco PR-15 mounting press. A GPX200 grinder/polisher was used to polish the samples
156 according to the standard sample preparation techniques (Taylor et al., 1998). A reflected light
157 microscope Leica DM 2500P linked to a TIDAS PMT IV photometric system was used to
158 determine petrographic composition of the samples by counting 500 points, and the results were

159 recalculated into volume percent. Representative photomicrographs were taken of each sample
160 using the same microscope. Coal, coke, tar and pitch, fly ash/bottom ash, sediments, and other
161 materials were the petrographic categories counted, and each category included several
162 components identified based on their optical characteristics.
163
164 2.7 Elemental analysis
165 The concentrations of selected elements were determined using a Thermo iCAP Qc inductively
166 coupled plasma mass spectrometry (ICP-MS, Thermo Fisher Scientific, Bremen, Germany). The
167 soil was extracted following EPA method 3050B, which is described in Hagmann et al. (2015).
168 Briefly, 5 mL of 50% HNO_3 was added to a 0.5 g homogenized sample. The solution was heated
169 to 95 ± 5 °C for 15 minutes. After the sample cooled down, 2.5 mL of concentrated HNO_3 was
170 added to the solution and the sample was heated 95 ± 5 °C for 30 minutes. This step was
171 repeated if brown fumes were present. Afterwards, the sample remained at 95 ± 5 °C until the
172 volume was reduced to approximately 2.5 mL. DI (1mL) water was then added to the solution
173 and drops of 30 % H_2O_2 (1.5 mL) were added. Further amounts of 30% H_2O_2 were added until
174 effervescence was minimal. The sample remained at 95 ± 5 °C until the volume dropped to 2.5
175 mL. The volume was brought up to 50 mL with DI water. The solution was then filtered
176 through a 1 μm filter. Each sample was further diluted to run on the ICP-MS. Samples were
177 diluted to at least 20 times to minimize the matrix effect. An aqueous standard curve was
178 prepared for Li, Mg, Al, P, K, Ca, Sc, V, Cr, Mn, Co, Ni, Cu, Zn, As, Mo, Ag, Cd, Ba and Pb
179 from a stock solution.
180
181

182 2.8 Acridine orange direct count (AODC)

183 Bacterial cell density was measured using epifluorescence microscopy after staining the soil
184 suspensions with acridine orange. Briefly, soil samples were suspended in phosphate buffered
185 saline (PBS) (0.0088 M Na_2HPO_4, 0.0013 M $NaH_2PO_4 \bullet H_2O$, 0.15 M NaCl; pH 7.6) and fixed
186 in formalin. The fixed samples were then serially diluted in PBS with a final dilution of 10^{-3}.
187 The diluted samples were then stained with 0.1 % acridine orange and transferred on a black
188 polycarbonate 0.2 μm IsoporeTM membrane filter (Millipore, Waltham, M.A.) and observed
189 under an epifluorescence microscope with a 100X objective lens (Nikon eclipse Ti-S) (Hobbie et
190 al. 1977, Krumins et al. 2009).

191

192 2.9 Phosphatase assay

193 Phosphatase enzyme activity was measured for soil from each site as described in Hagmann et al.
194 2015. Briefly, moist soil (0.1 g) was added to 100 mL of 0.1 M MES buffer (pH 6.0) and then
195 sonicated for 3 min at 25W. The slurry was stirred continuously, and each sample was added to
196 the well (160 μL). 4-MUB-phosphate was added (40 μL) to three different wells (350 μM in the
197 well). The concentration was determined by preparing a standard curve using different
198 concentrations of 4-MUB (0, 500, 1000, 1500 and 2500 pmols). Time points were collected on a
199 microplate reader at 30 °C every 20 minutes for 6 hours to measure fluorescence intensity (320
200 nm ex./450 nm em.).

201

202

203

204

205 **3. Results and discussion**

206 3.1. Bulk organic matter content

207 The soil from the reference site HMF has an organic matter content of 7.4 % (by LOI), similar to
208 typical forested soils in New Jersey (Table 1) (Osman, 2013). It should be noted that the solvent
209 extraction were conducted on soil particles that were less than 2 mm in diameter. In contrast,
210 forested LSP sites 43, 146, and 25F are unusually enriched in organic matter (30 - 45 %)
211 compared to typical New Jersey soils. Compared to the other LSP sites, the barren LSP site 25R
212 has a lower percentage of organic matter (10.8 %). The reference soil from HMF and barren 25R
213 soil have low solvent extract yields (1.3 and 1.2 g/kg_{soil}, respectively), compared to the forested
214 LSP sites 43, 146 and 25F, which yielded 7.3 to 9.8 g/kg_{soil}. Asphaltenes, higher molecular
215 weight compounds (500 - 1,000 or more Da) (Lewan et al., 2014), are dominant in the soils from
216 HMF and LSP sites 43, 146 and 25F, composing > 70 % of the extracts. Fraction 3
217 (predominantly polar compounds) is also prevalent (14 – 22 %) in these same soils (Table 1).
218 Site 25R is distinctive: in addition to the low extract yield, it contains only 47 % asphaltenes and
219 considerably more saturated hydrocarbons (Fraction 1, 17.6 %) than the other samples.

220 Table 1

221 The forested sites at LSP (43, 146 and 25F) contain both biological materials and
222 contaminants. The additional organic matter and extract yield in soils from these sites is likely
223 because of augmentation by fossil fuel materials. LOI measurements alone cannot distinguish
224 between coal and natural soil organic matter (Ball, 1964). However, we do indeed commonly see
225 chunks of coal in the LSP soils, which must obviously contribute to the elevated organic matter
226 at LSP. Samples HMF and 25R contain less soil organic matter and extract, but HMF is
227 forested, while 25R is barren (Fig. 1). The lower organic matter content and extract yield at 25R

Table 1. Organic matter content (%, mean ± SE; n = 3), extraction and liquid chromatographic results from HMF, 43, 146, 25F and 25R soils. Fraction 1 contains saturated hydrocarbons; fraction 2 – aromatic compounds and long chain (> C_{27}) normal alkanes; fraction 3 – polar compounds. The data show that soil from site 146 has the highest percent organic matter. The LC results show the percent of the total extract as well as yield per kg of dry soil.

Sample	Organic Matter (% of soil)	Extract yield (g/kg_{soil})	Fraction 1 mg/kg_{soil} (% of extract)	Fraction 2 mg/kg_{soil} (% of extract)	Fraction 3 mg/kg_{soil} (% of extract)	Asphaltenes mg/kg_{soil} (% of extract)
HMF	7.43 ± 0.63	1.28	43.0 (3.3)	52.0 (4.0)	287 (22.1)	918 (70.6)
LSP 43	29.8 ± 0.86	9.21	451 (4.9)	506 (5.5)	929 (10.1)	7,314 (79.5)
LSP 146	44.8 ± 2.18	9.83	549 (5.6)	451 (4.6)	1421 (14.5)	7,379 (75.3)
LSP 25F	31.6 ± 4.79	7.38	429 (5.8)	363 (4.9)	1,095 (14.8)	5,513 (74.5)
LSP 25R	10.8 ± 1.94	1.21	211 (17.6)	119 (9.9)	307 (25.6)	563 (46.9)

likely results from the lack of vegetation because plants provide constant organic inputs into the soil and obviously 25R soil does not receive these inputs. The organic matter content at HMF is normal for a forested soil and simply lacks the supplemental increment because of the contamination found at LSP. We note that the asphaltene contents of the forested LSP sites are high and further work must be done to characterize the asphaltenes, for example, by Py-GC-MS.

3.2. Py-GC-MS

Pyrolysis-GC-MS results (Table 2 and Fig. 3) showed that the reference site HMF contains organic compounds found in typical forest soils including lignin [L1], polysaccharide [P1, P2, P3, P4], and protein biomarkers [N2] (Fig. 3 A). Reference site HMF also contains low-weight aromatic hydrocarbons [A1, A2, A4] and phenols [F1, F2, F3, F4] (Fig. 3 A). Vegetated LSP sites 43, 146, and 25F contain the compounds present in HMF. These sites also contain PAHs such as naphthalenes and phenanthrenes, where both parent and alkylated forms are present, fluoranthene (Fig. 3 B), as well as dibenzofuran [DBF] and methyldibenzofuran [DBF1]. The chromatogram of barren LSP site 25R shows a notable absence of organic compounds with a biological derivation [e.g., L1, L2 etc.] and thus predominantly aromatic compounds are seen in the trace. The aromatic compounds seen at site 25R are also present in similar proportions at the other LSP sites (Fig. 3).

Table 2

Figure 3

The presence of polysaccharides, lignin, and proteins in HMF was expected because these compounds indicate plants and microorganisms in the soil (*e*.g. Hempfling and Schulten, 1990). These compounds are also present in vegetated LSP sites 43, 146, and 25F but not at

Fig. 3. Total ion current (TIC) for Py-GC-MS of soil samples from sites HMF (A), 43 (B), 146 (C), 25F (D) and 25R (E). The data for 25R show predominantly mono- and polycyclic aromatic hydrocarbons and aromatic hydrocarbons. See Table 2 for compound symbols.

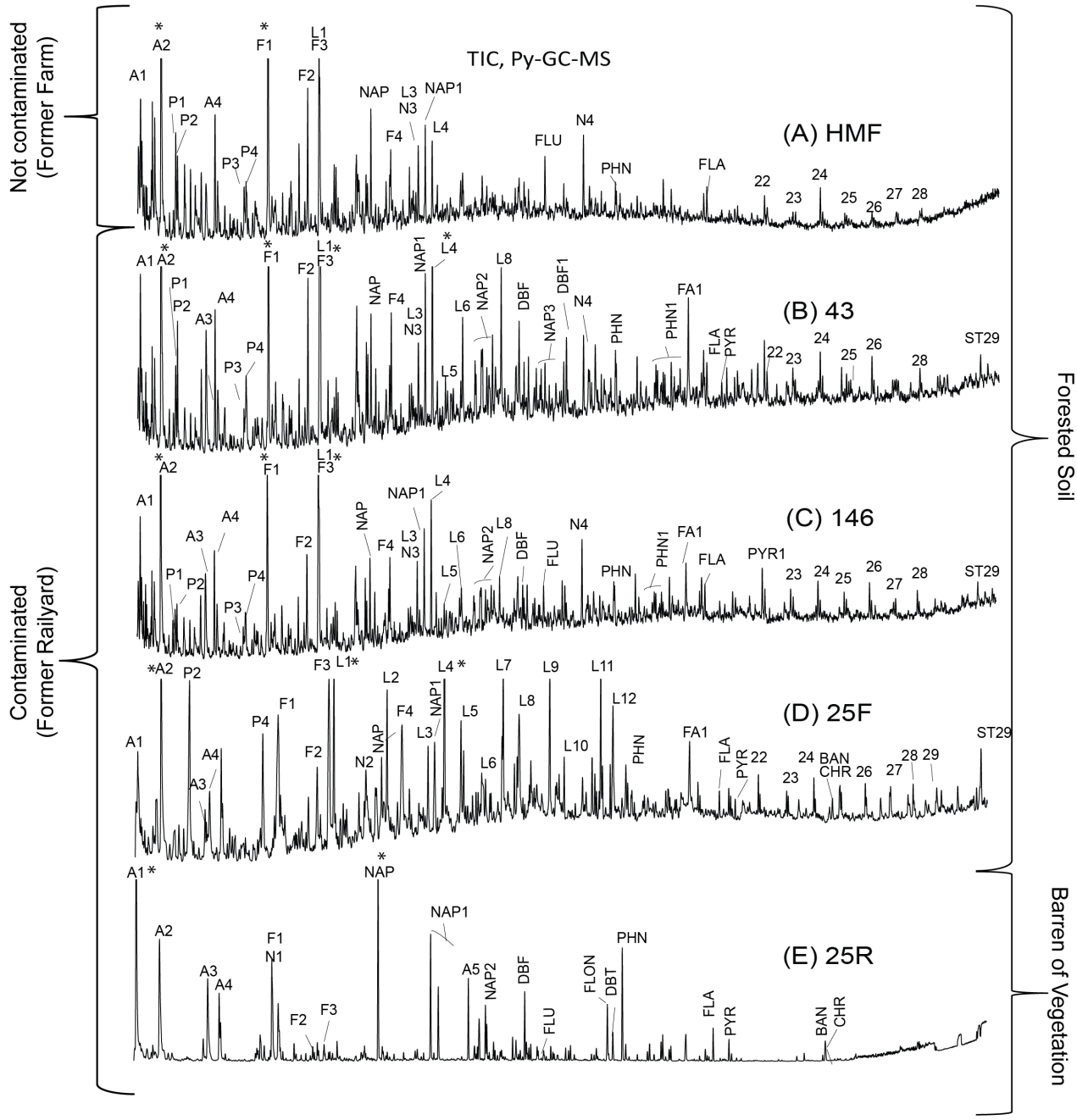


Table 2: Symbols for peak identification used in Figures 1-7.

Aliphatic Hydrocarbons	
Numerals	normal alkanes
Pr	pristane
Ph	phytane
Hx	hopanes (x is the carbon number)
Ts	18α(H)-22,29,30-trisnorhopane
Tm	17α(H)-22,29,30-trisnorhopane
TRx	tricyclic terpane
Aromatic Compounds	
Alkylated aromatic compounds, "x" is degree of substitution	
A1	benzene
A2	toluene
A3	m-xylene & p-xylene
A4	styrene
A5	biphenyl
NAP	naphthalene
NAPx	alkylnaphthalene isomers
PHN	phenanthrene
PHNx	alkylphenanthrene isomers
ANT	anthracene
FLA	fluoranthene
FLU	fluorene
FLON	9H-fluoren-9-one
PYR	pyrene
PYRx	alkypyrene isomers
CHR	chrysene
CHRx	alkylchrysene isomers
BAN	benzo[*a*]anthracene
BNT	benzonapthothiophene
BFLA	benzofluorene
DBF	dibenzofuran
DBFx	alkyldibenzofuran isomers
DBT	dibenzothiophene
Polysaccharide Marker Compounds	
P1	cyclopentenone
P2	furfural
P3	3-methylcyclopentenone
P4	methylfurfual
P5	levoglucosan
Phenolic Compounds	
F1	phenol
F2	2-methylphenol
F3	3-methylphenol & 4-methylphenol
F4	vinylphenol

Table 2. (continued)	
Lignin Marker Compounds	
L1	guaiacol
L2	methylguaiacol
L3	ethylguaiacol
L4	vinylguaiacol
L5	syringol
L6	vanillin
L7	trans iso-eugenol
L8	acetovanillone
L9	vinylsyringol
L10	prop-1-enyl syringol
L11	prop-2-enyl syringol (trans)
L12	acetosyringone
Fatty Acid	
FA1	*n*-hexadecanoic acid
FA2	*n*-octadecanoic acid
FA3	methyl ester (E) 9-octadecanoic acid
FA4	octadecanoic acid, butyl ester
Nitrogen Compounds	
N1	benzonitrile
N2	benzeneacetonitrile
N3	indole
N4	diketodipyrole
Steroid	
S1	C29 steradiene
S2	cholest-5-en-3-ol
S2	ergost-5-en-3-ol
S3	γ-stigmasterol
S4	stigmast-5-en-3-ol
S5	stigmastanol
S6	stigmast-4-en-3-one
Plasticizer	
X1	diisobutyl phthalate
X2	1,2-benzenedicarboxylic acid, bis(2-ethylhexyl) ester
Other Compounds	
B1	abietane derivative
B2	β-amyrin derivative
B6	diploptene
B13	totarol
B14	1-heptacosanol
B15	3β-methoxy-D-friedoolean-14-ene
B16	olean-12-en-3-one
B17	lupeol
B18, B19	dammarane isomers
B20	cyclolaudenol
B21	lup-20(29)-ene-3,28-diol

barren site 25R. The pyrolyzates of the LSP sites 43, 146 and 25F soils have similar organic compositions to each other, which is not surprising because they are all vegetated and located within the same brownfield. The PAHs present at LSP sites indicate fossil fuel contamination and include naphthalenes, fluoranthene, and fluorene, and heterocyclic compounds, such as dibenzofuran. One likely source is coal, particles of which are evident to the naked eye in the park soils, and it is known that the presence of coal in the soil can increase the amount of aromatic compounds including PAHs (Kögel-Knabner, 2000; Laumann et al., 2011; Nádudvari et al., 2018; Stout and Emsbo-Mattingly, 2008).

One example of coal indicators include dibenzofuran and methyldibenzofuran (Nádudvari et al., 2018). In contrast to the other sites, 25R pyrolyzate shows a strong predominance of aromatic compounds. These aromatic compounds include monoaromatic hydrocarbons such as BTEX (benzene [A1], toluene [A2], ethylbenzene, xylene [A3]) and polycyclic aromatic hydrocarbons (PAHs) [NAP, PHN, FLA, PYR, CHR, BAN]. Compared to the other LSP sites, the different organic composition at site 25R can be largely attributed to the absence of plants at 25R. Organic compounds at forested LSP soils come from vegetation or industrial sources and compounds originating from plants can obscure signatures of contaminants (Ortiz et al., 2016b). With many of the plant and microbial indicators missing, the PAH indicators are more clearly visible in the 25R total ion current (TIC) trace. Our findings indicate that the organic contaminant profile of site 25R is similar to the other LSP sites. This suggests that the lack of plants at site 25R is not a result of differences in organic contaminant composition.

3.3. Solvent extractable organic matter

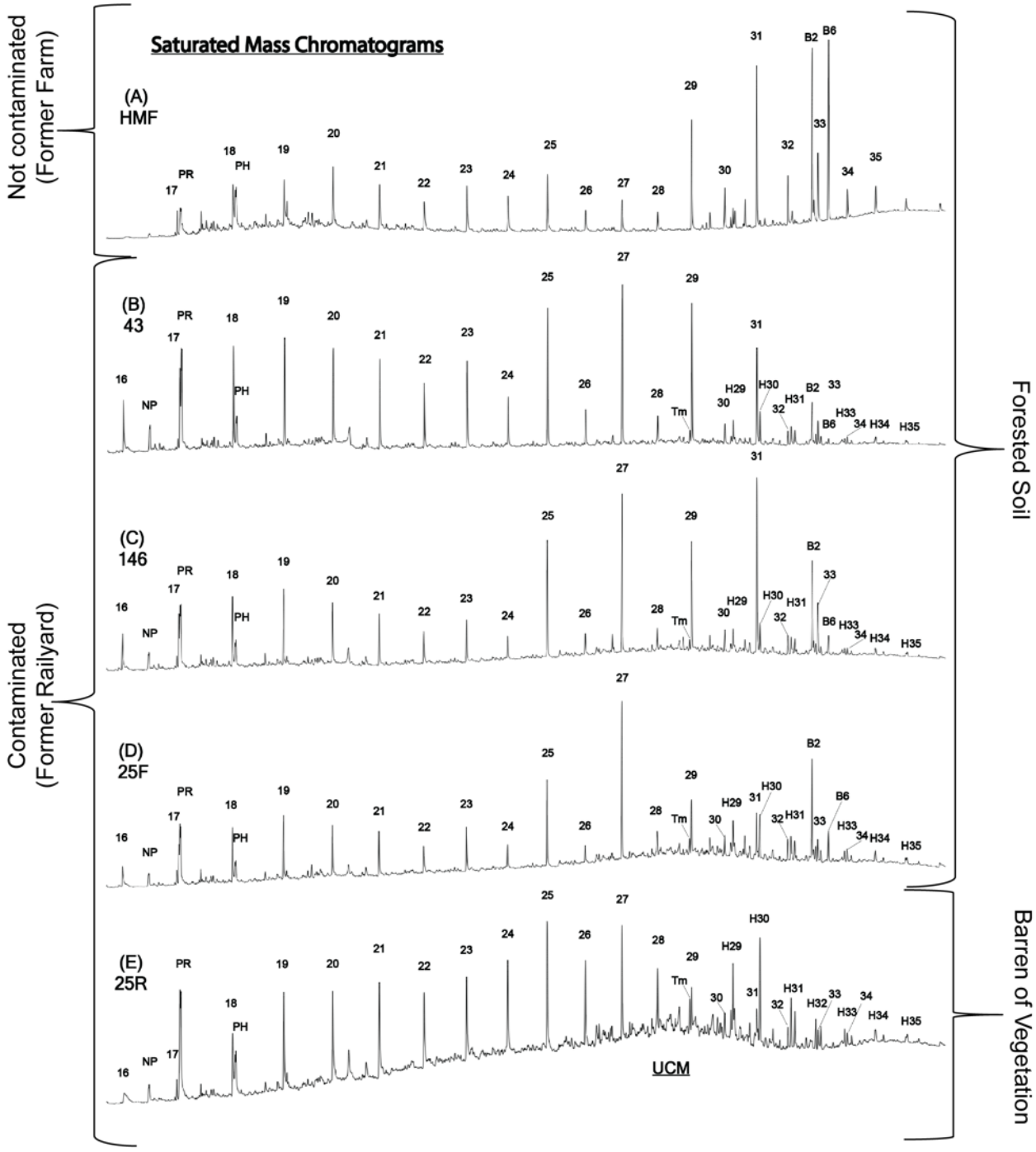
3.3.1. Fraction 1 (saturated hydrocarbons)

The saturated chromatograms (Fig. 4) contain two different sub-groups, normal isoprenoids (m/z 71) and triterpenoids (m/z 191). The distributions of saturated hydrocarbons indicate that the soil of reference site HMF soil is distinctly different from soils from the four LSP sites (Fig. 4, Supp. Fig. S1). The HMF samples show a predominance of two higher plant triterpenoid biomarkers, diploptene [B2] and a β-amyrin derivative [B6] as well as the long-chain, odd carbon number alkanes *n*-C_{29} and *n*-C_{31} (Figs. 4A and 5A). For soil samples 43, 146, and 25F, we see a lower relative abundance of the two biomarkers [B2] and [B6] compared to HMF and a broader range of odd-carbon number *n*-alkanes ($C_{24} - C_{31}$) (Fig. 4B-D, Fig. 5 B-D and Supp. Fig. S1). The $C_{27} - C_{35}$ triterpenoid and isoprenoid alkanes are prominent in soils 43 and 146 (Fig. 4 B-D). The chromatogram for barren site 25R shows a distinctive "baseline hump", indicating an unresolved complex mixture (UCM) of hydrocarbons (Fig. 4 E). Hopanes are relatively more abundant in site 25R compared to the other sites, however, the biomarkers [B2] and [B6] are not detected (Fig. 4 E).

Figure 4

There is notably more pristane [Pr] than phytane [Ph] at all LSP sites having pristane/phytane (Pr/Ph) ratios of *ca*. 3. In LSP soils, pristane was found more abundant than *n*-C_{17} and phytane was found to be less abundant than *n*-C_{18} (Fig. 4, Table 3, Supp. Fig. S1). Hopanes (m/z 191) are key compounds found in contaminated LSP sites (Fig. 5) and were not found in the reference site HMF (Fig. 5 A). Soils from 25R do not show the biomarkers [B2] and [B6], likely owing to the absence of plant biomass or low numbers of soil microbes.

Fig. 4. Total ion current (TIC) for fraction 1 of soil extracts from sites HMF (A), 43 (B), 146 (C), 25F (D) and 25R (E). The data show distributions of alkanes (normal isoprenoids (m/z 71) and triterpenoids (m/z 191). See Table 2 for compound symbols.



297 Table 3

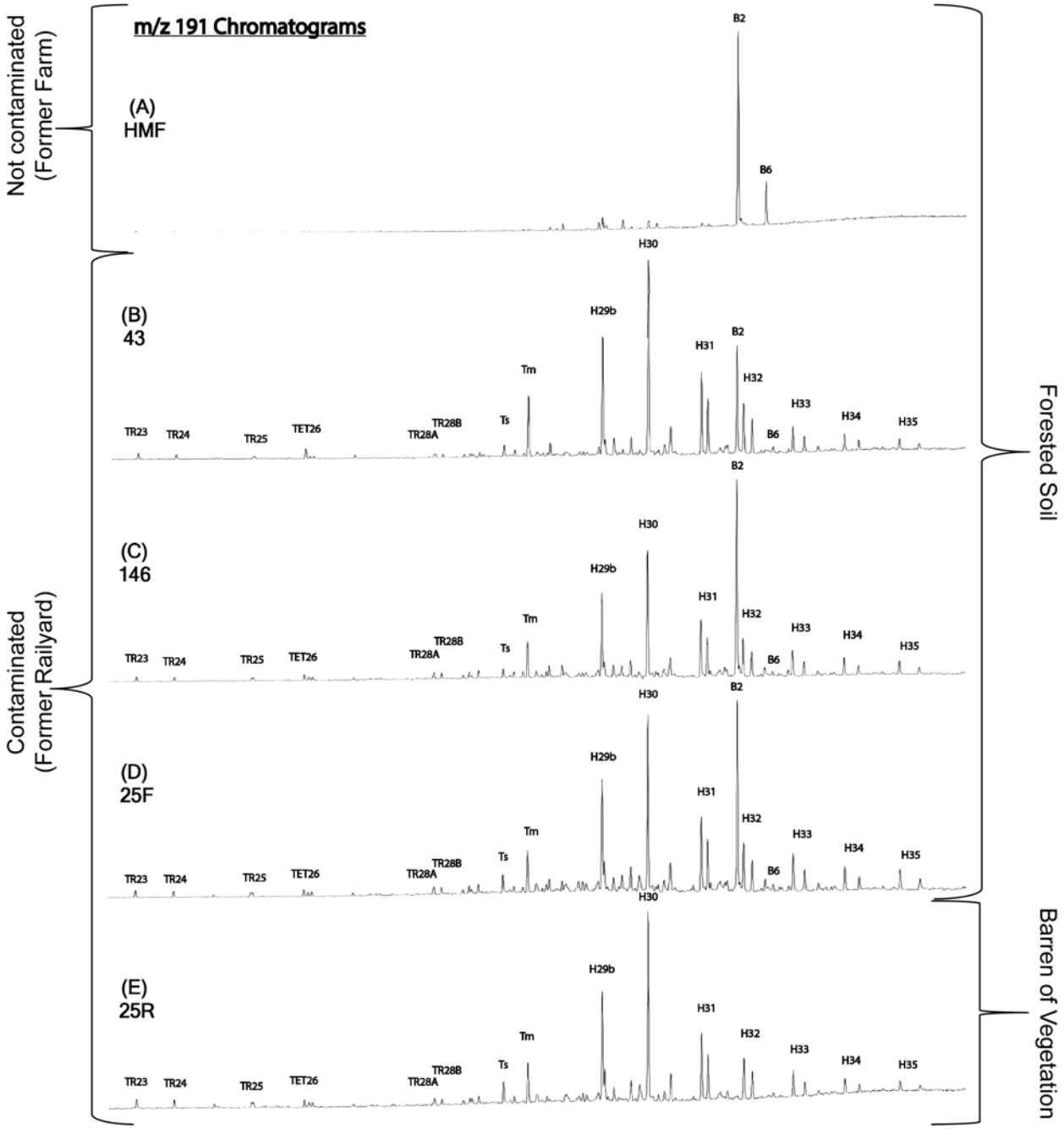
298 Figure 5

299 The presence of pristane, phytane, hopanes, tricylclic terpanes, sesquiterpanes and
300 steranes in LSP soils indicates fossil fuel contamination (Fig. 4, Supp. Fig. S2 and S3) (Killops
301 and Killops, 2005; Peters et al., 2005; Wang and Fingas, 2003; Wang and Stout, 2010; Wang et
302 al., 2005). The distribution of these compounds is similar in all samples analyzed, which
303 indicates a similar blend of contaminating hydrocarbons at the four LSP sites. Hopanes, clearly
304 visible in Figures 4 and 5, suggest the presence of heavy petroleum products such as fuel or
305 lubricating oil in addition to coal (Peters et al., 2005). The reference site HMF does not contain
306 hopanes, consistent with HMF soils containing less contamination compared to LSP. These
307 findings support our first hypothesis that we will find more fossil fuel contaminants in LSP
308 compared to HMF. The reference site HMF also yielded less of Fraction 1 (43.0 mg/kg_{soil})
309 compared to all LSP sites, where yields range from 211-549 mg/kg_{soil}. The high Pr/Ph ratios at
310 LSP sites (> 2.7) are consistent with the presence of bituminous coal (Table 3) (Peters et al.,
311 2005; Powell and McKirdy, 1973). The main railroad lines through sites 146 and 43 transported
312 coal from Pennsylvania to a coal pier to go to New York City (Fig. 1) (Caldes, 2010; French,
313 2002). Other railroad lines were directed to sites 25R and 25F and carried other cargo, however
314 all railroad tracks had locomotives that could spill coal. Our C_{27}-C_{28}-C_{29} sterane ternary diagram
315 pairs sites based on proximity to each other, for example, soils from sites 43 and 146 have higher
316 abundance of C_{29} compared to soils from 25R and 25F (Supp. Fig. S4) (Peters et al., 2005). The
317 GC-MS data on the saturated fraction reflects the presence of both coal and petroleum products
318 at LSP.

Table 3. Carbon preference index (CPI), odd even predominance (OEP), pristine/phytane (Pr/Ph), Pr/C17, Ph/C18, and weighted average carbon number of HMF, 43, 146, 25F and 25R are shown.

Sample	CPI	OEP	Pr/Ph	Pr/C17	Ph/C18	weighted average carbon number
HMF	2.573	2.782	0.634	2.464	2.137	26.33
43	4.726	4.480	3.533	2.667	0.539	23.82
146	6.770	6.689	2.720	2.430	0.635	25.23
25F	4.067	4.877	2.960	3.576	0.689	24.53
25R	1.533	1.225	3.148	11.853	1.264	23.80

Fig. 5. Mass chromatogram (m/z 191) showing the distribution of hopanes and tricyclic terpanes in the saturated fractions. The β-amyrin derivative is a soil microbe biomarker that was observed in all sites except for 25R. See Table 2 for compound symbols.



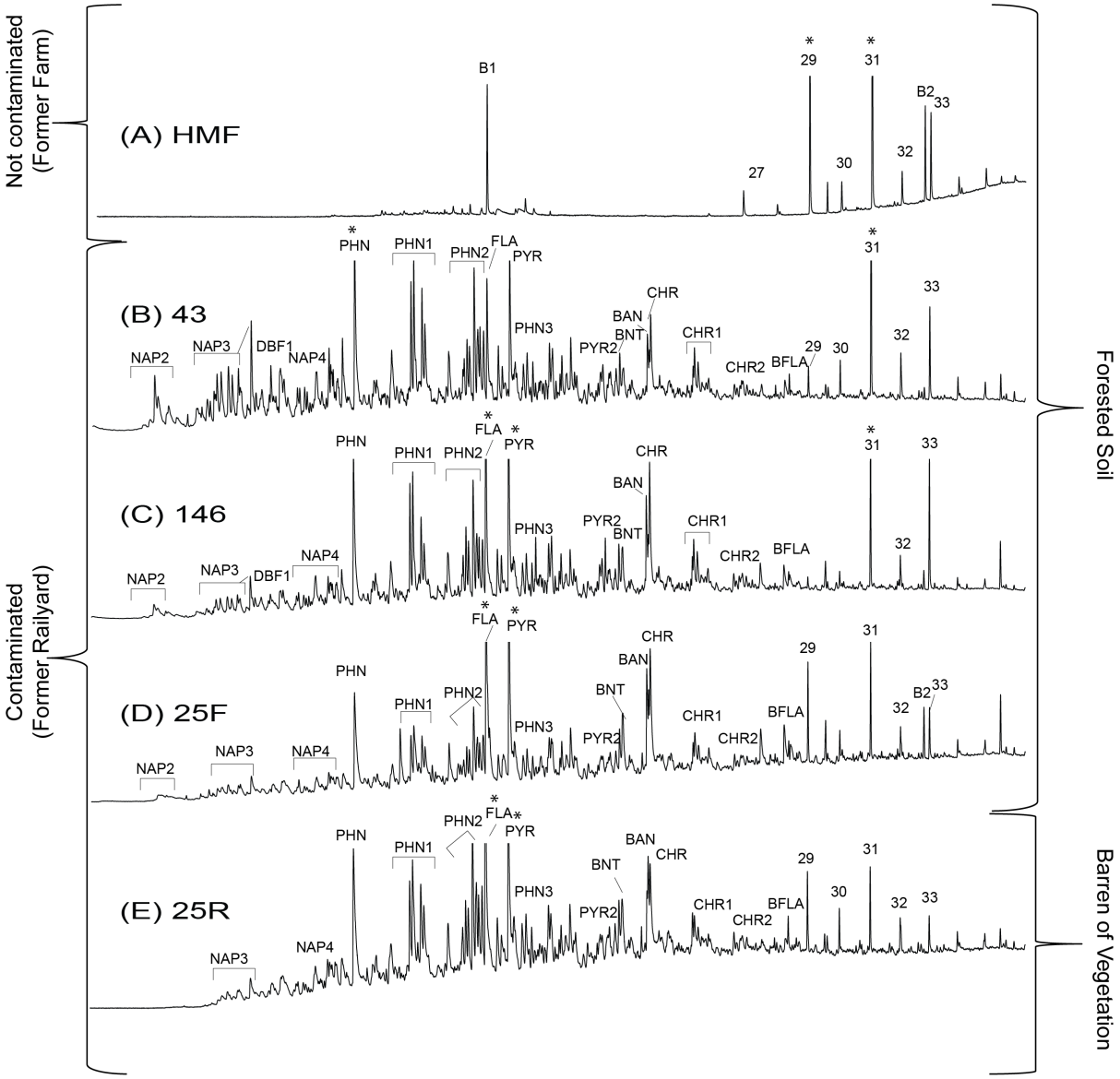
An odd-even predominance (OEP) is observed for HMF and the forested LSP soils, especially in extracted m/z 71 (Fig. 4 and Supp. Fig. S1), reflecting the presence of higher plants, specifically plant waxes. The triterpenoid biomarkers [B2] and [B6] are chemical signatures of soil microbes and are seen in HMF and forested LSP soils. Not surprisingly, soils from barren site 25R do not display OEP or biomarkers [B2] or [B6], consistent with the site's lack of vegetation (Fig. 4). Within LSP, site 25R has higher isoprenoid to normal alkane ratios (pristane/*n*-C17 and phytane/*n*-C18) compared to the other sites. This can be explained by preferential biodegradation of *n*-alkanes compared to the isoprenoids at some point in the site's history (Table 3) (Peters et al., 2005). Biodegradation at site 25R is also supported by the UCM as seen in Figure 4E. This is surprising because site 25R supports no vegetation. It is possible that microbial degradation of fossil fuels at site 25R took place at the time of contamination and the signs we observe are from an earlier period of degradation.

3.3.2. Fraction 2 (aromatic hydrocarbons)

Soil extract from the reference site HMF had lower amounts of Fraction 2 (predominantly aromatic hydrocarbons) (52.0 mg/kg_{soil}) than did LSP soil extracts (Table 1). For the forested LSP sites, extract Fraction 2 values ranged from 363 to 506 mg/kg_{soil} while LSP soil 25R yielded somewhat less than the other LSP sites, 119 mg/kg_{soil} of extract Fraction 2. We intended for the LC separation to segregate saturated hydrocarbons into Fraction 1 and aromatic compounds into Fraction 2 but some long chain aliphatic hydrocarbons (> C_{27}) also eluted into Fraction 2 (Fig. 6). We observed only one major aromatic compound in the solvent extract from the uncontaminated reference site HMF (Fig. 6 A), which is an abietane derivative [B1]. In the extracts from LSP, the primary aromatic compounds are PAHs (Fig. 6 B - E) and include parent

342 and alkylated napthalenes, phenanthrenes, pyrenes, chrysenes and their isomers [e.g. NAPx,
343 PHN, PYR, CHR]. Also notable in LSP soils are heterocyclic compounds including
344 dibenzofurans and benzonaphthothiophene [DBF, BNT]. Sample 25R's PAH distributions
345 resemble those in the other LSP samples but there is also a noticeable UCM (Fig. 6 E).
346 Figure 6
347 The aromatic fraction data indicate that the chosen reference soil HMF is indeed relatively
348 uncontaminated while all LSP sites have significant PAH contamination. These data also
349 support our hypothesis that there are more fossil fuel biomarkers present at LSP compared to
350 HMF. The overall aromatic hydrocarbon distribution is similar for all LSP soils (Fig. 6 B-E),
351 reflecting similar mixtures of contaminants. Fraction 2 data for LSP 25R soil indicated a
352 significant UCM, which suggests weathering and biodegradation, in agreement with Fraction 1
353 data (Figs. 4 E, 6 E). If biodegradation is taking place, we might expect the concentration of low
354 weight molecular PAHs, like naphthalene, to decrease (Biache et al., 2017). We observe PAHs in
355 our data; perhaps these compounds are absorbed in coal particles and thus shielded from
356 biodegradation (Liu et al., 2008). We note that the PAH distributions in the pyrolyzates of the
357 LSP soils and extracted Fraction 2 show a greater predominance of parent PAHs than those of
358 the extract (Fraction 2), as seen by comparison of Figure 3E with 6E and specifically with PHN
359 in Supplemental Fig. S5 (Wang and Fingas, 2003). The greater predominance of parent
360 compounds indicates a pyrogenic source, which derives from incomplete combustion of fossil
361 fuels (Chen et al., 2004; Given, 1987; Micić et al., 2011; Stout and Emsbo-Mattingly, 2008).
362
363 3.3.3. Fraction 3 (polar compounds)
364 The soil from the reference site HMF contains ergosterol and stigmasterol derivatives [S2, S3,
365 S4, S5, S6], a diterpenoid tentatively identified as totarol [B13], and octadecanoic acid butyl

Fig. 6. Total ion current (TIC) for fraction 2 of soil extracts from the HMF (A), 43 (B), 146 (C), 25F (D) and 25R (E) sites. The data show fewer polycyclic aromatic hydrocarbons in HMF. Distributions of aromatic compounds are similar for chromatograms B, C, D, and E. See Table 2 for compound symbols.

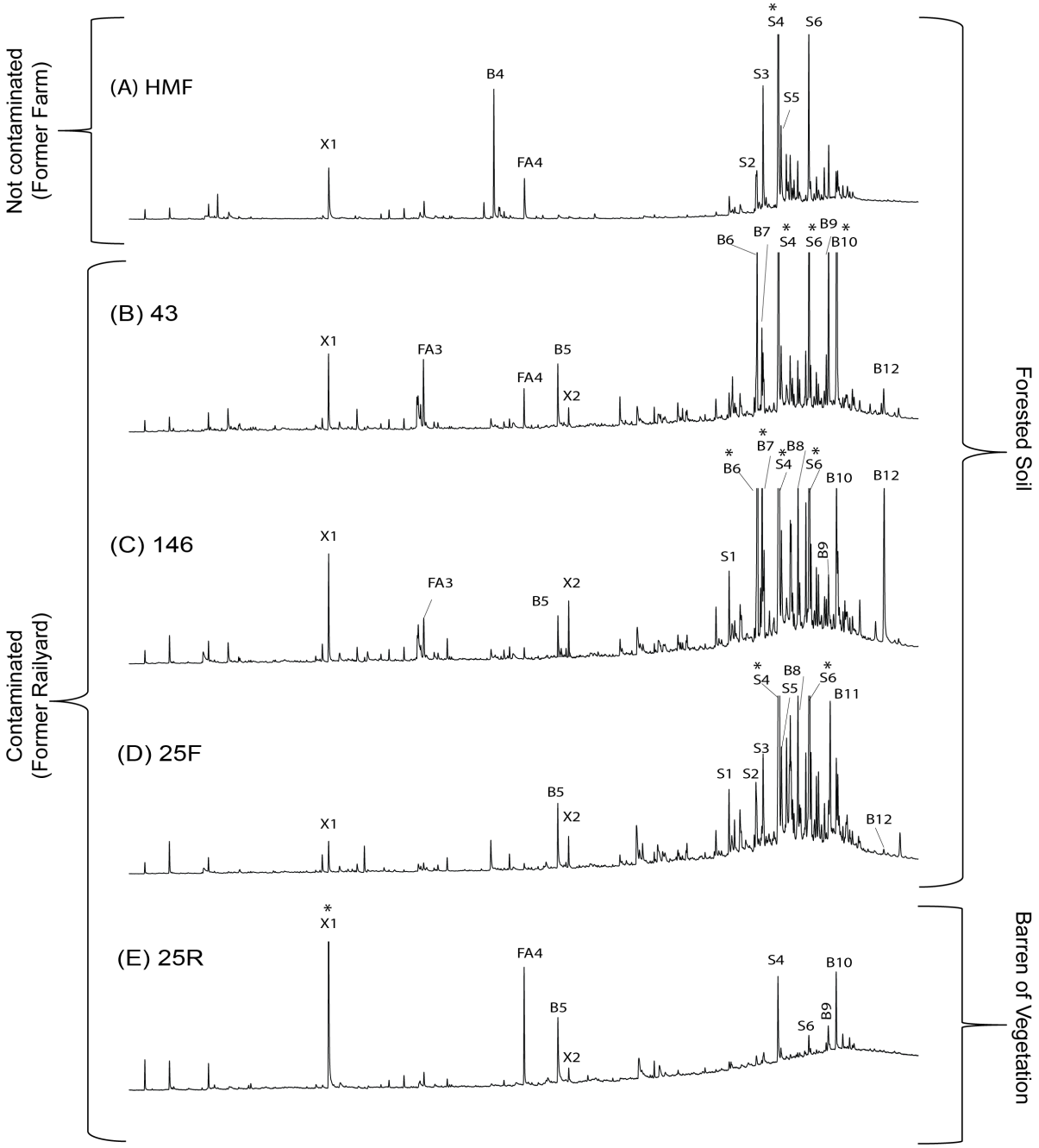


ester [FA4] (Fig. 7 A). This ester and the steroids are also present in the forested soils from LSP (Fig. 7 B-D). The plasticizer, diisobutyl phthalate [X1], is present in all soils. Compounds present in all LSP sites, but not in HMF, include 1-heptacosanol and 1,2-benzenedicarboxylic acid, bis(2-ethylhexyl) ester [B14, X2]. The triterpenoids tentatively identified as 3β-methoxy-D-friedoolean-14-ene and olean-12-en-3-one [B15, B16] were present in LSP 43 and 146 soils, while lupeol and lup-20(29)-ene-3,28-diol [B17, B21] were found in LSP 146 and 25R soils (Fig. 7 B-D). LSP site 25R has fewer polar compounds compared to the other sites but includes the steroids stigmast-5-en-3-ol and stigmast-4-en-3-one [S4, S6] (Fig. 7 E).

Figure 7

The soil at HMF contains both ergosterol and stigmasterol derivatives. Ergosterols are generally found in fungi, while stigmasterol typically occurs in higher plants (Peters et al., 2005). HMF also contains totarol [B13], which is a cyclic diterpenoid that is present in resins from higher plants (Tinoco et al., 2006), and a long chain alcohol, 1-heptacosanol, which is present in terrestrial organic matter (Wang et al., 2009; Yunker et al., 1995). All of these compounds are compatible with a normal, temperate forest soil. The vegetation present at HMF is predominantly cedar. The plasticizer diisobutyl phthalate [X1] is present in all the studied soils, possibly a result of having stored the soil samples in plastic bags. The origin of octadecanoic acid butyl ester in soils is of unknown origin and could be another plasticizer introduced during sample handling (Cahill et al., 2006). The dominant species present at LSP is *Betula populifolia*, which is present at 43, 146 and 25F (Evans et al., 2015; Gallagher et al., 2008b). Lupeol [B8] and lup-20(29)-ene-3,28-diol [B12] are biological indicators of birch (Peters et al., 2005). The microbially and plant-derived steroids and triterpenoids are much less abundant at site 25R, not unexpected since it is void of vegetation. The presence of life in 25R is also apparent in the

Fig. 7. Total ion current (TIC) for fraction 3 of soil samples from the HMF (A), 43 (B), 146 (C), 25F (D) and 25R (E). See Table 2 for compound symbols.



389 polar compounds, specifically sitosterol (stigmast-5-en-3-ol) and the degradation product of
390 sitosterol, stigmast-4-en-3-one (Mackenzie et al., 1982; Pautler et al., 2013).

391 3.4. Organic petrography

392 All samples (soil particles smaller than 2 mm) from LSP had high amount of organic matter and
393 it was represented dominantly by anthropogenic material. Coal particles were prominent in all
394 four samples, accounting for 14.3 to 30.0 vol. %, and they were especially abundant in samples
395 25R and 43. Coal particles were of various ranks from high volatile bituminous to anthracite,
396 with the latter being the dominant rank in all samples (Fig. 8). Carbonization-derived material
397 (coke) is also common and ranges from 6.6 to 12.0 vol. %, with samples 43 and 146 having the
398 largest proportions (Fig. 8 and 9). Tar and pitch-like material were prominent in samples 25R
399 and 25F (Figs. 8 and 9), and far less abundant in the other two samples. Combustion-derived
400 material accounted for 7.1 to 23.1%, being most common in sample 146 (Fig. 8). The
401 combustion-derived material was represented both by organic material (char) and mineral matter
402 (glass, spinel, etc.) (Fig. 9). In total, anthropogenic material accounted for more than 50 vol % of
403 all the samples with site 25R soil having the largest contribution (Fig. 8). Recent organic matter
404 (classified as "other" in Fig. 8) was rare and represented by wood fragments.

405 Figure 8

406 Figure 9

407 Organic petrography was useful in comparing LSP sites in terms of soil organic
408 components, including different ranks of coal, coke, tar and pitch, fly ash/bottom ash, sediments,
409 and other materials (Suárez-Ruiz et al., 2012). The organic petrography profiles of sites close to
410 each other at LSP share similarities; for example, soils from 43 and 146 that are located close in
411 proximity and are along train tracks to a coal pier based on historic aerial photographs (Fig. 1B)

Fig. 8. Organic petrographic composition (in volume %) of samples 43, 146, 25F and 25R. The data show that 25F and 25R have more tar/pitch compared to 43 and 146. HMF soil was not analyzed for organic petrography because coal particles were not visible to the naked eye.

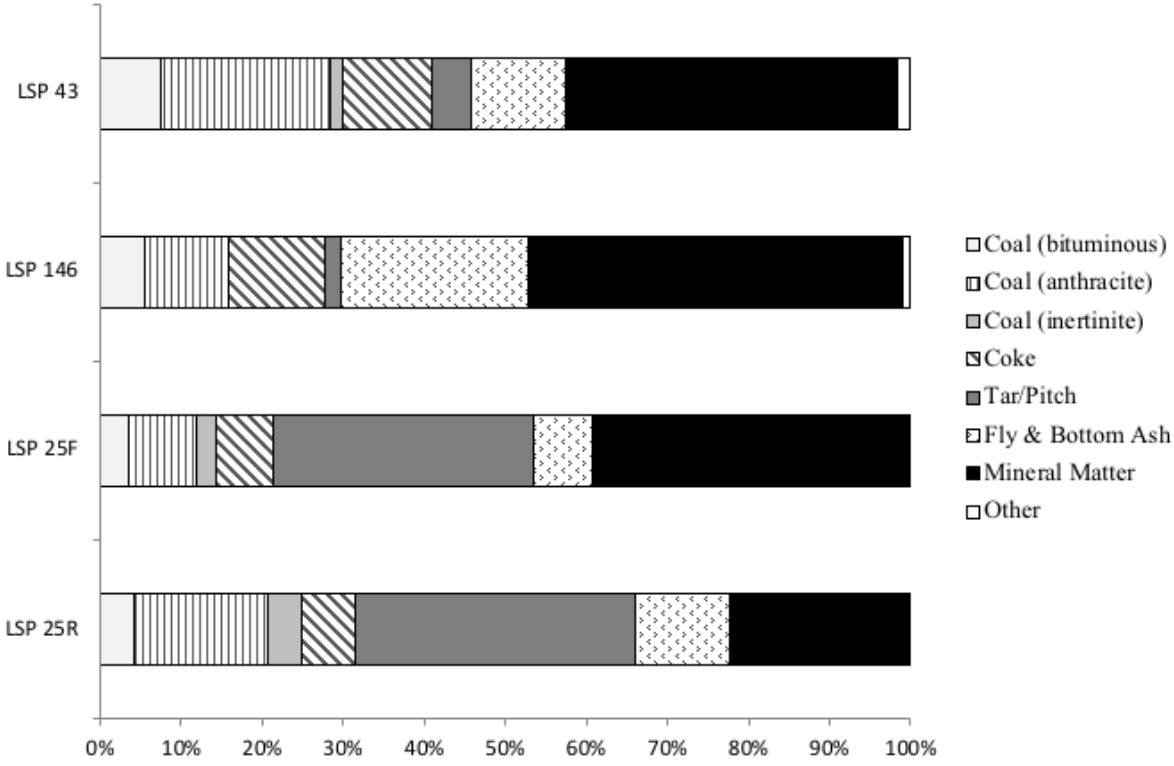
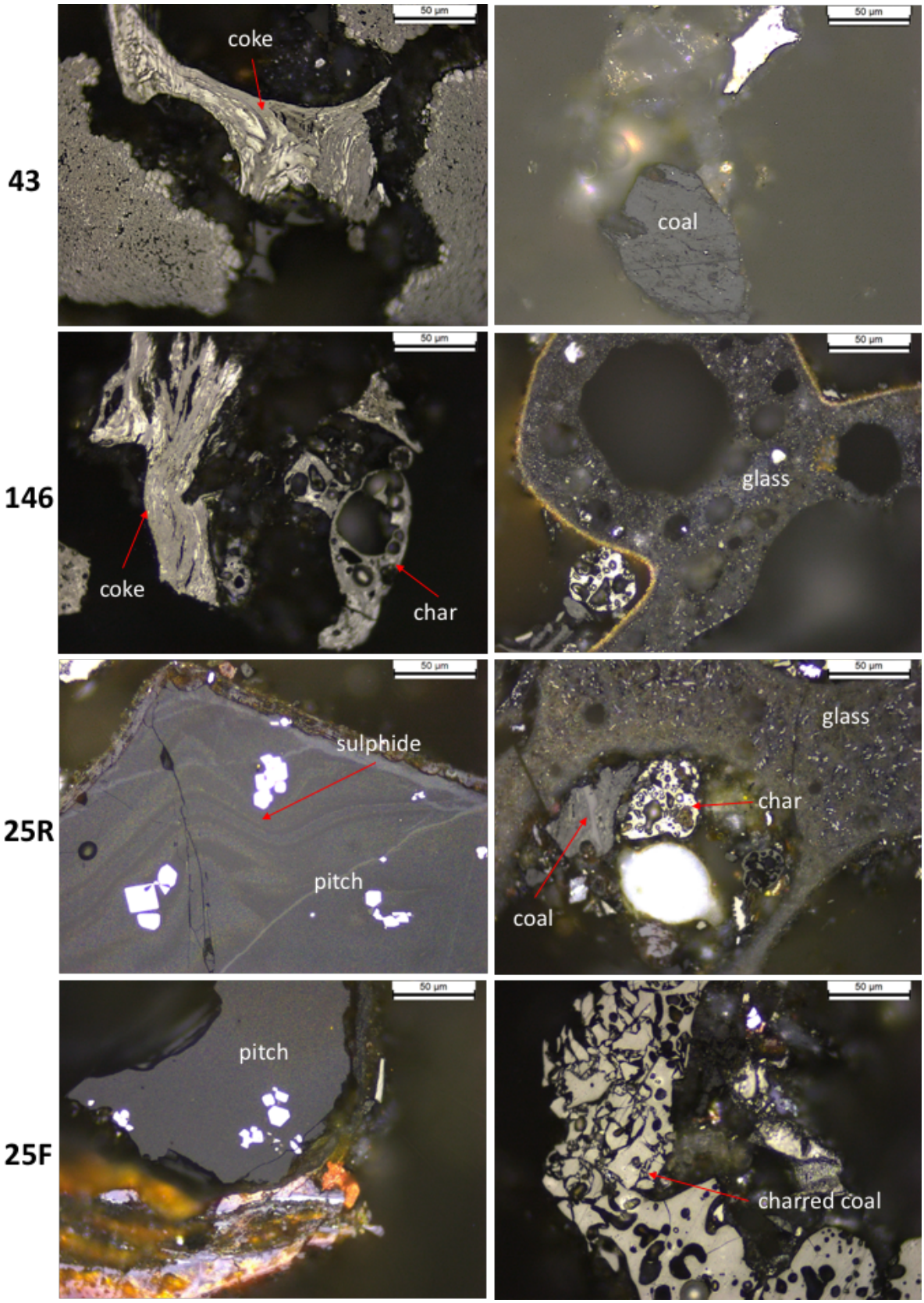


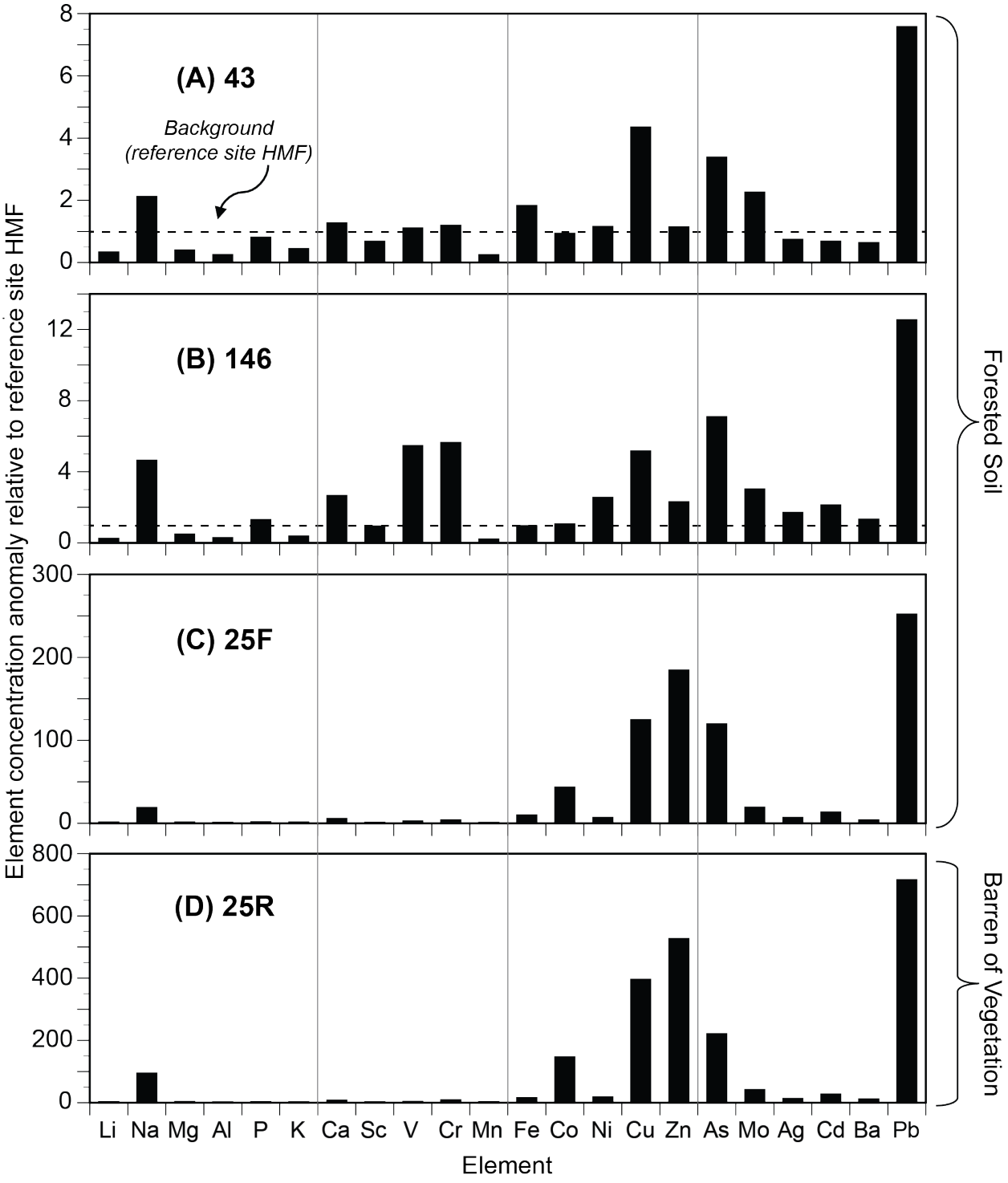
Fig. 9. Examples of photomicrographs of anthropogenic particles identified in the samples. Each sample has two photomicrographs. Reflected light, oil immersion.



412 have the highest abundance of coke. Soils from 25F and 25R, which are adjacent sites, were
413 both prominent in tar and pitch-like material. Site 25R has the largest proportion of non-mineral
414 material (Fig. 8), which could be a reason for or the result of a lack of vegetation at this site.
415
416 3.5. Inorganic elemental analysis
417 The concentrations of several inorganic compounds in HMF and LSP soils were also determined
418 (Supp. Table S1). As expected, we found the lowest concentrations of metals (V, Cr, Ni, Cu, Zn,
419 As, and Pb) at the reference site HMF; however, HMF soil showed a high Al concentration
420 (20,527 ± 249 ppm), which was matched by only one of the LSP sites, 25R (Supp. Table S1).
421 There were elevated concentrations of Na, Co, Cu, Zn, As, and Pb at both 25F ([Na]: 873; [Co]:
422 256; [Cu]: 2256; [Zn] 14435; [As] 630; [Pb] 7145 mg/kg, triplicate measurements, see Supp.
423 Table S1 for errors) and 25R ([Na]: 4393; [Co]: 869; [Cu]: 7165; [Zn] 41271; [As]: 1162; [Pb]
424 20302 mg/kg) compared to the other LSP sites (Supp. Table S1).
425 Sanders (2003) in a survey of New Jersey soils, determined background levels of metals;
426 the HMF metal concentrations closely match his values from northeastern New Jersey ("urban
427 Piedmont") soils (Supp. Table S1) (Sanders, 2003), confirming that HMF is a good reference soil
428 for this study. The high concentrations of Al in HMF relative to LSP soils may suggest a higher
429 abundance of aluminosilicate clay minerals in HMF compared to LSP (Barton et al., 2002;
430 Buettner and Valentine, 2011). Figure 10 shows element concentration anomalies at LSP sites;
431 metal concentrations were normalized to the reference site HMF values. Specifically, we find
432 anomalously high levels of Na, Co, Cu, Zn, As, and Pb in LSP soils, especially at sites 25F and
433 25R (Fig. 10). For example, As concentrations in 25F and 25R were found to be 119 and 220
434 times higher compared to HMF, respectively. Although these sites are adjacent, As

435 concentrations are about two times higher at 25R compared to 25F. It is common to find As, Cr,
436 Cu, Pb and Zn in contaminated soil. In particular, As, Cu, Cr, and Zn are associated with
437 chromated copper arsenate, which was used in some rail yards for treating wood used for railroad
438 ties (Kumpiene et al., 2008). Another possible explanation for the anomalously high
439 concentrations is that bulk minerals, perhaps pyrites, sulfides, or oxides, were transported on the
440 railroad lines, possibly supplying not only Fe but also As, Cd, Co, Cu, and Ni (Finkelman, 1995).
441 It is also possible that coal and slag, which can include the trace elements in coal ashes, were
442 transported through LSP (Schweinfurth, 2003).
443 Figure 10
444
445 3.6 Extracellular soil phosphatase activities and bacterial density
446 Site 146 has the highest bacterial density (cells/$g_{dry\ soil}$) (7.87 (± 0.82) × 10^8) of the sites (Fig. 11
447 A). Soils from HMF (4.64 (± 0.93) × 10^8), 43 (4.37 (± 0.35) × 10^8), and 25F (4.97 (± 0.61) ×
448 10^8) are forested and have similar bacterial densities to each other. The barren site 25R has
449 lower but measurable bacterial density (2.09 (± 0.76) × 10^8 cells/$g_{dry\ soil}$). The data in Figure 11 B
450 show that site 146 has the highest phosphatase activity (2.60 (± 0.55) × 10^6 pmol/g/h) of the soils
451 studied here. This result agrees with previous findings where we found that site 146 has higher
452 phosphatase, cellobiohydrolase and L-leucine-amino peptidase activities compared to three other
453 LSP sites and to HMF (Hagmann et al., 2015). Despite the measurable bacterial density, the
454 phosphatase activity at barren 25R is below the threshold of detection. It is surprising that site
455 25F, which is located next to site 25R, has high phosphatase activity (pmol/g/h) (1.38 (± 0.39) ×
456 10^6). The phosphatase activities at HMF and 43 are (0.47 (± 0.38) × 10^6) and (0.67 (± 0.13) ×
457 10^6), respectively.

Fig. 10 Concentrations elements listed in order of atomic weight normalized to HMF. The data is arranged from the lowest to the highest (43, 146, 25F and 25R) average metal concentration. The dotted line present in A. and B. is the background HMF.

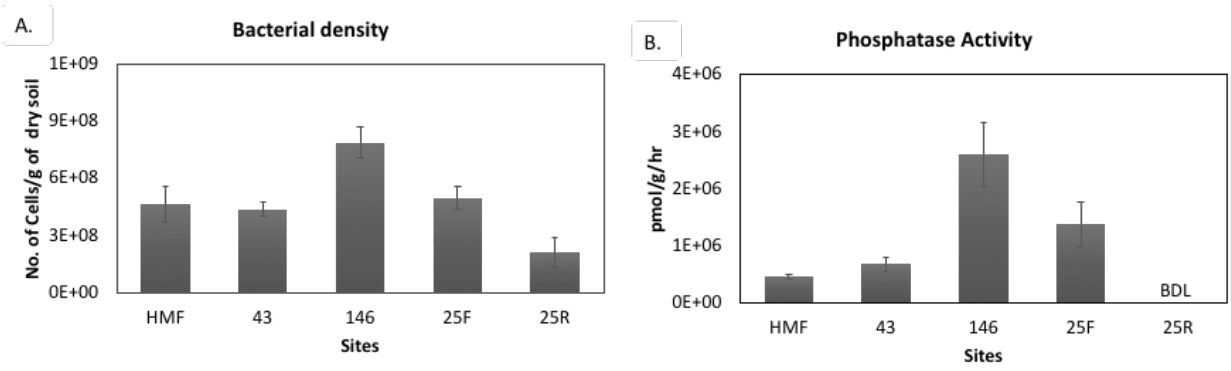


458 Figure 11

459 The low but measurable bacterial density we found at barren site 25R indicates the
460 presence of bacterial life. Even so, the phosphatase activity in the soil is below the threshold of
461 detection and it is possible the bacteria in 25R soil are dormant, perhaps owing to poor nutrient
462 cycling and availability. In a previous study, Singh and co-workers found via next-generations
463 sequencing that the bacterial community at site 25R is statistically distinct from the other LSP
464 sites (Singh et al., 2019b). The presence of bacteria in 25R soil is consistent with the
465 biodegradation at this site discussed in Section 3.3.1. It is possible that microbial degradation of
466 fossil fuels indicated by the UCM in the 25R GC-MS data took place at some time in the site's
467 history.

468 Site 146 has high bacterial density and phosphatase activity (Fig. 11) and also the highest
469 percent organic matter (44 %) (Table 1). We had originally hypothesized that the high function
470 at site 146 is due to differences in organic compound profiles, perhaps because of the absence of
471 specific contaminants that are present at other LSP sites. Conversely, we found that site 146 has
472 an organic composition similar to the other forested sites at LSP as seen in the pyrolysis and GC-
473 MS data (Figs. 3, 4, 5, and 6); however, organic composition may not explain the high activity at
474 this site. Site 25R is also distinct from the other LSP sites: it has no plants and no detectable
475 phosphatase activity. If this absence of function is a result of organic contaminants, we would
476 expect to observe differences in the organic contaminant profiles between site 25R and the other
477 LSP sites. Analogously to site 146, we found that the organic composition at site 25R is similar
478 to the other sites at LSP as seen in the pyrolysis and GC-MS data except that compounds
479 associated with higher plants are absent (Figs. 3, 4, 5, and 6).

Fig. 11. Bacterial density (cells/g dry soil, mean and error bars are SE; n = 3) and phosphatase activity (pmol*g^{-1}*hr^{-1}, mean and error bars are SE; n =3) of HMF, 43, 146, 25F, and 25R soils are shown.



We considered the possibility that the low function at 25R is due not to differences in the identity of organic contaminants but rather the concentration of specific compounds in the soil. This is unlikely because the extract yields from 25R for soil particles less than 2 mm in diameter are significantly lower than for the other LSP sites. These data together suggest that the organic contaminant profile at site 25R is not responsible for the functional differences between this site and other LSP sites. Previous findings by Singh et al. (2019a) showed that abiotic factors are more important than biotic ones for enzymatic function in LSP soils. In light of these findings and having now ruled out a different organic contaminant profile as the reason for the low function at site 25R, our new hypothesis is that the higher concentrations of Na, Co, Cu, Zn, As, and Pb at 25R (discussed in Section 3.5) are responsible for the poor function of the site (Singh et al., 2019a). The concentrations of these metals are about 2 to 5 times higher than in the forested and high functioning site 25F that is located adjacent to site 25R. We plan to further investigate whether these elevated metal concentrations at 25R affect soil extracellular enzymatic activity and plant production. For example, it is possible that the As concentrations at site 25R are sufficiently high to inhibit phosphatase activity (Lee et al., 2011; Lorenz et al., 2006; Speir et al., 1999).

3.7 Insights into functional variation between LSP sites

All LSP sites are contaminated with PAHs and other fossil fuel-derived components that are absent or barely detectable at reference site HMF. The presence of the PAHs, hopanes, steranes, and sesquiterpanes supports our first hypothesis that there are more fossil fuel biomarkers at LSP compared to HMF. Vegetated sites at LSP have unnaturally high organic matter content (30 to 45 %), relative to pristine vegetated soils, reflecting large quantities of anthropogenic

503 contaminants in these soils. The distributions of the PAHs and fossil fuel biomarkers are similar
504 for all soils within LSP. However, the yield of extractable organic matter at 25R is lower and
505 thus we suspect that the extraordinarily high content of *inorganic* contaminants rather than
506 organic contaminants explains the barren site's lack of vegetation. We hypothesized that the
507 barren site 25R would have more or different contaminants compared to the forested sites at
508 LSP. This was found to be true for several inorganic contaminants but not for the organic
509 contaminant profiles within LSP.

510 LSP's history and the soils' chemical and petrographic fingerprints agree with the
511 location of the sites within the rail yard. Sites 43 and 146 are located on what was once a dense
512 array of railroad tracks leading to the coal pier. Their soils contain more coal and less tar and
513 pitch compared to sites 25F and 25R, which were on different railroad lines carrying other
514 unspecified cargo. We observe wider gaps between tracks in historical photographs of the 25F
515 and 25R area, in which we suspect that dumping activities occurred (Fig. 1 D and E). It is
516 possible that 25F is forested and has high phosphatase activity, because it was on an active
517 railroad track whereas 25R was on a gap, where more dumping occurred, and thus has low
518 phosphatase activity. While we did not find evidence that would explain these differences in the
519 nonbiologically-derived organic contaminant profiles, we note significantly higher metal
520 contaminant concentrations in 25R compared to 25F.

521

522 3.8 Implications for investigating contaminated ecosystems

523 In this study, we used several experimental methods in conjunction with pyrolysis GC-MS to
524 study soils from three types of sites: an uncontaminated vegetated reference site (HMF),
525 contaminated vegetated sites (LSP 43, 146, 25F) and a contaminated, industrial barren (25R).

526 Our data are consistent with the presence and absence of biologically derived organic matter in
527 the study sites: biological pyrolysis products are not present in the organic chemical fingerprint
528 of soil 25R, which instead shows a predominance of contaminant-derived aromatic compounds.
529 These data serve as a case study or reference set for the differences in data observed for
530 contaminated vegetated and contaminated barren soils, especially because indicators from
531 vegetation can chemically obscure the signatures of contaminants.
532 Site 25R in LSP is an example of an area that is contaminated and barren as a result of
533 past anthropogenic activities and, possibly, the subsequent environmental and physical
534 conditions. Such "industrial barrens" are present worldwide and are considered "extreme
535 environments" (Kozlov and Zvereva, 2007). Unfortunately, industrial barrens, and especially
536 those that have high heavy metal loads, are often unlikely to recover naturally but, even so, they
537 are studied less than other extreme environments. Many studies on industrial barrens focus on
538 evaluation of damage and development of rehabilitation measures while more fundamental
539 studies on soil function and detailed soil characterization are lacking, limiting our understanding
540 of the fundamental chemistry, biochemistry and ecology of these sites. Kozlov and Zvereva
541 (2007) suggested that researchers often choose the most contaminated but planted sites within an
542 area for their studies because they are more comparable with less disturbed sites.
543
544 4. Conclusion
545 Site 25R is an example of an industrial barren and here we have conducted a multifaceted
546 chemical and biochemical analysis of this soil and compared the findings to those in nearby
547 vegetated sites. The phosphatase activity at site 25R is below our limit of detection, yet direct
548 bacterial counts indicate the presence of bacteria. Interestingly, these findings suggest that

549 microbes in 25R soils are present but lying dormant, perhaps as a result of either inorganic
550 contaminant loads or physical abiotic restrictions in the soil. Perhaps fostering plant growth,
551 aerating the soil, or adding root exudates to the contaminated 25R soil will revive some of the
552 microbes and subsequently improve nutrient cycling and overall soil function. The inactive
553 microorganisms may be waiting for an environmental nudge or input to revitalize them and
554 unleash their functional potential in the currently contaminated, poorly functioning, and barren
555 25R soil. This same story of dormant and abiotically limited microbes, waiting to be revitalized,
556 may be playing out in other industrial barrens throughout the world. It behooves the scientific
557 community to more fully investigate these sites to obtain a deeper and more fundamental
558 understanding, which can then be leveraged to prevent land degradation and to restore
559 dysfunctional and phytotoxic soils.
560

561 **Acknowledgements**

562 We thank the National Science Foundation (NSF CBET 1603741) and the PSEG Institute for
563 Sustainability Studies for the support for this study. We thank Gregory Pope for valuable
564 discussions during the project. Finally, we thank Frank Gallagher for facilitating access to
565 Liberty State Park.
566

Figure and Table Caption

Fig. 1. Liberty State Park is located in Jersey City, New Jersey (A). Aerial images from: U. S. Geological Survey: 1954 (B, E) and 2014 (C). Study sites within LSP are indicated on the map (43, 146, 25F, 25R). A historical photograph of 25F and 25R from 1951 (D). Sites 25F and 25R are adjacent; 25R is in a strip of land without vegetation (F). Photo credits: D: Andrew Bologovsky, F: Mike Peters (Montclair State University). Photos used with permission.

Fig. 2. Flow chart illustrating the experimental design for the experiment.

Fig. 3. Total ion current (TIC) for Py-GC-MS of soil samples from sites HMF (A), 43 (B), 146 (C), 25F (D) and 25R (E). The data for 25R show predominantly mono- and polycyclic aromatic hydrocarbons and aromatic hydrocarbons. See Table 2 for compound symbols.

Figure 4. Total ion current (TIC) for fraction 1 of soil extracts from sites HMF (A), 43 (B), 146 (C), 25F (D), and 25R (E). The data show distributions of alkanes (normal isoprenoids (m/z 71) and triterpenoids (m/z 191). See Table 2 for compound symbols.

Figure 5. Mass chromatogram (m/z 191) showing the distribution of hopanes and tricyclic terpanes in the saturated fractions. The β-amyrin derivative is a soil microbe biomarker that was observed in all sites except for 25R. See Table 2 for compound symbols.

Fig. 6. Total ion current (TIC) for fraction 2 of soil extracts from the HMF (A), 43 (B), 146 (C), 25F (D), and 25R (E) sites. The data show fewer polycyclic aromatic hydrocarbons in HMF. Distributions of aromatic compounds are similar for chromatograms B, C, D, and E. See Table 2 for compound symbols.

Fig. 7. Total ion current (TIC) for fraction 3 of soil samples from the HMF (A), 43 (B), 146 (C), 25F (D) and 25R (E). See Table 2 for compound symbols.

Fig. 8. Organic petrographic composition (in volume %) of samples 43, 146, 25F, and 25R. The data show that 25F and 25R have more tar/pitch compared to 43 and 146. HMF soil was not analyzed for organic petrography because coal particles were not visible to the naked eye.

Fig. 9. Examples of photomicrographs of anthropogenic particles identified in the samples. Each sample has two photomicrographs. Reflected light, oil immersion.

Fig. 10. Element concentration anomalies relative to reference site HMF. Elements are presented in order of atomic weight, with each normalized to its value in the HMF reference soil. The plots are arranged from the lowest (site 43) to the highest (25R) overall metal concentration. The dotted lines visible in A and B show the background HMF values.

Fig. 11. Bacterial density (cells/g dry soil, mean and error bars are SE; n = 3) and phosphatase activity ($pmol*g^{-1}*hr^{-1}$, mean and error bars are SE; n =3) of HMF, 43, 146, 25F, and 25R soils are shown.

Table 1. Organic matter content (%, mean ± SE; n = 3), extraction and liquid chromatographic results from HMF, 43, 146, 25F and 25R soils. Fraction 1 contains saturated hydrocarbons; fraction 2 – aromatic compounds and long chain (> C_{27}) normal alkanes; fraction 3 – polar compounds. The data show that soil from site 146 has the highest percent organic matter. The LC results show the percentage of the total extract as well as yield per kg of dry soil.

Table 2: Symbols for peak identification used in Figures 1-7.

Table 3. Carbon preference index (CPI), odd-even predominance (OEP), pristine/phytane (Pr/Ph), Pr/C17, Ph/C18, and weighted average carbon number of HMF, 43, 146, 25F and 25R.

634

635 **References**

636 Alisi C., Musella R., Tasso F., Ubaldi C., Manzo S., Cremisini C., et al., 2009. Bioremediation of
637 diesel oil in a co-contaminated soil by bioaugmentation with a microbial formula tailored
638 with native strains selected for heavy metals resistance. Sci. Total Environ.; 407: 3024-
639 3032.
640 Alker S., Joy V., Roberts P., Smith N., 2000. The Definition of Brownfield. J. Environ. Plann.
641 Man.; 43: 49-69.
642 Ball D., 1964. Loss- on- ignition as an estimate of organic matter and organic carbon in
643 non- calcareous soils. J. Soil Sci.; 15: 84-92.
644 Baran S., Bielińska J.E., Oleszczuk P., 2004. Enzymatic activity in an airfield soil polluted with
645 polycyclic aromatic hydrocarbons. Geoderma; 118: 221-232.
646 Biache C., Ouali S., Cébron A., Lorgeoux C., Colombano S., Faure P., 2017. Bioremediation of
647 PAH-contamined soils: Consequences on formation and degradation of polar-polycyclic
648 aromatic compounds and microbial community abundance. J. Hazard Mater.; 329: 1-10.
649 Brooks K.M., 2004 Polycyclic aromatic hydrocarbon migration from creosote-treated railway
650 ties into ballast and adjacent wetlands. Madison, WI: U.S. Department of Agriculture,
651 Forest Service, Forest Products Laboratory.
652 Buettner K.M., Valentine A.M., 2011. Bioinorganic chemistry of titanium. Chem. Rev.; 112:
653 1863-1881.
654 Cahill T.M., Seaman V.Y., Charles M.J., Holzinger R., Goldstein A.H., 2006. Secondary organic
655 aerosols formed from oxidation of biogenic volatile organic compounds in the Sierra
656 Nevada Mountains of California. J. Geophys Res Atmos; 111.
657 Caldes C., 2010 Jersey City's Hudson River Waterfront Book Two: Lehigh Valley, Central
658 Railroad of New Jersey, Erie, DL&W, Erie-Lackawanna 1941-1964. Vol 2: Journal
659 Square Publishing.
660 Chen Y., Bi X., Mai B., Sheng G., Fu J., 2004. Emission characterization of particulate/gaseous
661 phases and size association for polycyclic aromatic hydrocarbons from residential coal
662 combustion. Fuel; 83: 781-790.
663 Evans J.M., Parker A., Gallagher F., Krumins J.A., 2015. Plant Productivity, Ectomycorrhizae,
664 and Metal Contamination in Urban Brownfield Soils. Soil Sci.; 180: 198-206.
665 Finkelman R.B., 1995. Modes of Occurrence of Environmentally-Sensitive Trace Elements in
666 Coal. In: Swaine DJ, Goodarzi F, editors. Environmental Aspects of Trace Elements in
667 Coal. Springer Netherlands, Dordrecht, pp. 24-50.
668 French K., 2002 Railroads of Hoboken and Jersey City. Charleston, SC: Arcadia Publishing.
669 Gallagher F.J., Pechmann I., Bogden J.D., Grabosky J., Weis P., 2008a. Soil metal
670 concentrations and productivity of Betula populifolia (gray birch) as measured by field
671 spectrometry and incremental annual growth in an abandoned urban Brownfield in New
672 Jersey. Environ. Pollut.; 156: 699-706.
673 Gallagher F.J., Pechmann I., Bogden J.D., Grabosky J., Weis P., 2008b. Soil metal
674 concentrations and vegetative assemblage structure in an urban brownfield. Environ.
675 Pollut.; 153: 351-361.

676 Gallego J., Rodríguez-Valdés E., Esquinas N., Fernández-Braña A., Afif E., 2016. Insights into a
677 20-ha multi-contaminated brownfield megasite: an environmental forensics approach.
678 Sci. Total Environ.; 563: 683-692.
679 Given P., 1987. The mobile phase in coals: its nature and modes of release. Final report–Part 2.
680 Efforts to Better Define the Nature and Magnitude of the Mobile Phase. Prepared for the
681 US Department of Energy. DOE-PC-60911-F2., pp. 42.
682 Hagmann D.F., Goodey N.M., Mathieu C., Evans J., Aronson M.F.J., Gallagher F., et al., 2015.
683 Effect of metal contamination on microbial enzymatic activity in soil. Soil Biol.
684 Biochem.; 91: 291-297.
685 Hamdi H., Benzarti S., Manusadžianas L., Aoyama I., Jedidi N., 2007. Bioaugmentation and
686 biostimulation effects on PAH dissipation and soil ecotoxicity under controlled
687 conditions. Soil Biol. Biochem.; 39: 1926-1935.
688 Haritash A., Kaushik C., 2009. Biodegradation aspects of polycyclic aromatic hydrocarbons
689 (PAHs): a review. J. Hazard. Mater.; 169: 1-15.
690 Hempfling R., Schulten H.R., 1990. Chemical characterization of the organic matter in forest
691 soils by Curie point pyrolysis-GC/MS and pyrolysis-field ionization mass spectrometry.
692 Org. Geochem.; 15: 131-145.
693 Jackson D.P., 1997. Evaluation of ex-situ soil washing as a remedial strategy for heavy metal
694 removal from railyard ballast. Hazardous and Industrial Wastes; 29: 158-164.
695 Killops S., Killops V., 2005 Introduction to Organic Geochemistry. Oxford: Blackwell
696 Publishing.
697 Kögel-Knabner I., 2000. Analytical approaches for characterizing soil organic matter. Org.
698 Geochem.; 31: 609-625.
699 Kozlov M.V., Zvereva E.L., 2007. Industrial barrens: extreme habitats created by non-ferrous
700 metallurgy. Rev. Environ. Sci. Bio.; 6: 231-259.
701 Kruge M., 2015. Analytical pyrolysis principles and applications to environmental science.
702 Environmental Applications of Instrumental Chemical Analysis, CRC Press, Boca Raton,
703 FL: 533-569.
704 Kruge M.A., Gallego J.L.R., Lara-Gonzalo A., Esquinas N., 2018. Chapter 7 - Environmental
705 Forensics Study of Crude Oil and Petroleum Product Spills in Coastal and Oilfield
706 Settings: Combined Insights From Conventional GC–MS, Thermodesorption–GC–MS,
707 and Pyrolysis–GC–MS. In: Stout SA, Wang Z, editors. Oil Spill Environmental Forensics
708 Case Studies. Butterworth-Heinemann, pp. 131-155.
709 Kumpiene J., Lagerkvist A., Maurice C., 2008. Stabilization of As, Cr, Cu, Pb and Zn in soil
710 using amendments – A review. Waste Manag.; 28: 215-225.
711 Lacey R.F., Cole J.A., 2003. Estimating water pollution risks arising from road and railway
712 accidents. Q. J. Eng. Geol. Hydroge.; 36: 185.
713 Lara-Gonzalo A., Kruge M.A., Lores I., Gutiérrez B., Gallego J.R., 2015. Pyrolysis GC–MS for
714 the rapid environmental forensic screening of contaminated brownfield soil. Org.
715 Geochem.; 87: 9-20.
716 Laumann S., Micić V., Kruge M.A., Achten C., Sachsenhofer R.F., Schwarzbauer J., et al., 2011.
717 Variations in concentrations and compositions of polycyclic aromatic hydrocarbons
718 (PAHs) in coals related to the coal rank and origin. Environ. Pollut.; 159: 2690-2697.
719 Lee S.-H., Kim E.Y., Park H., Yun J., Kim J.-G., 2011. In situ stabilization of arsenic and metal-
720 contaminated agricultural soil using industrial by-products. Geoderma; 161: 1-7.

721 Lewan M.D., Warden A., Dias R.F., Lowry Z.K., Hannah T.L., Lillis P.G., et al., 2014.
722 Asphaltene content and composition as a measure of Deepwater Horizon oil spill losses
723 within the first 80days. Org. Geochem.; 75: 54-60.
724 Liu H., Chen L.-P., Ai Y.-W., Yang X., Yu Y.-H., Zuo Y.-B., et al., 2008. Heavy metal
725 contamination in soil alongside mountain railway in Sichuan, China. Environ. Monit. and
726 Assess; 152: 25.
727 Lorenz N., Hintemann T., Kramarewa T., Katayama A., Yasuta T., Marschner P., et al., 2006.
728 Response of microbial activity and microbial community composition in soils to long-
729 term arsenic and cadmium exposure. Soil Biol. Biochem.; 38: 1430-1437.
730 Mackenzie A.S., Brassell S.C., Eglinton G., Maxwell J.R., 1982. Chemical Fossils: The
731 Geological Fate of Steroids. Science; 217: 491.
732 Malawska M., Wilkomirski B., 1999. An analysis of polychlorinated biphenyls (PCBs) content
733 in soil and plant leaves (taraxacum officinale) in the area of the railway junction Iława
734 Główna AU -. Toxicol. Environ. Chem.; 70: 509-515.
735 Malawska M., Wiłkomirski B., 2000. Soil and plant contamination with heavy metals in the area
736 of the old railway junction Tarnowskie Góry and near two main railway routes. Rocz
737 Panstw Zakl Hig; 51: 259-267.
738 Malawska M., Wiołkomirski B., 2001. An Analysis of Soil and Plant (Taraxacum Officinale)
739 Contamination with Heavy Metals and Polycyclic Aromatic Hydrocarbons (PAHs) In the
740 Area of the Railway Junction Iława Główna, Poland. Water Air Soil Pollut.; 127: 339-
741 349.
742 Maliszewska-Kordybach B., Smreczak B., 2003. Habitat function of agricultural soils as affected
743 by heavy metals and polycyclic aromatic hydrocarbons contamination. Environ. Int.; 28:
744 719-728.
745 Micić V., Kruge M.A., Köster J., Hofmann T., 2011. Natural, anthropogenic and fossil organic
746 matter in river sediments and suspended particulate matter: A multi-molecular marker
747 approach. Sci. Total Environ.; 409: 905-919.
748 Nádudvari Á., Fabiańska M.J., Marynowski L., Kozielska B., Konieczyński J., Smołka-
749 Danielowska D., et al., 2018. Distribution of coal and coal combustion related organic
750 pollutants in the environment of the Upper Silesian Industrial Region. Sci. Total
751 Environ.; 628-629: 1462-1488.
752 Ortiz J.E., Borrego Á.G., Gallego J.L.R., Sánchez-Palencia Y., Urbanczyk J., Torres T., et al.,
753 2016a. Biomarkers and inorganic proxies in the paleoenvironmental reconstruction of
754 mires: The importance of landscape in Las Conchas (Asturias, Northern Spain). Org.
755 Geochem.; 95: 41-54.
756 Ortiz J.E., Sánchez-Palencia Y., Torres T., Domingo L., Mata M.P., Vegas J., et al., 2016b. Lipid
757 biomarkers in Lake Enol (Asturias, Northern Spain): Coupled natural and human induced
758 environmental history. Org. Geochem.; 92: 70-83.
759 Osman K.T., 2013. Organic Matter of Forest Soils. Forest Soils: Properties and Management.
760 Springer International Publishing, Cham, pp. 63-76.
761 Pautler B.G., Sanborn P.T., Simpson A.J., Simpson M.J., 2013. Molecular characterization of
762 organic matter in Canadian Arctic paleosols for paleoecological applications. Org.
763 Geochem.; 63: 122-138.
764 Peters K.E., Peters K.E., Walters C.C., Moldowan J., 2005 The biomarker guide. Vol 1:
765 Cambridge University Press.

766 Powell T.G., McKirdy D.M., 1973. Relationship between Ratio of Pristane to Phytane, Crude Oil
767 Composition and Geological Environment in Australia. Nature-Phys Sci.; 243: 37.
768 Qian Y., Gallagher F., Deng Y., Wu M., Feng H., 2017. Risk assessment and interpretation of
769 heavy metal contaminated soils on an urban brownfield site in New York metropolitan
770 area. Environ. Sci. Pollut. R.; 24: 23549-23558.
771 Sanders P.F., 2003. Ambient levels of metals in New Jersey soils. Environmental Assessment
772 and Risk Analysis Element Research Project Summary. New Jersey Dept. of
773 Environmental Protection, Division of Science, Research & Technology, Trenton, N.J.
774 Schweinfurth S.P., 2003 Coal--a Complex Natural Resource: An Overview of Factors Affecting
775 Coal Quality and Use in the United States. Vol 1143: US Department of the Interior, US
776 Geological Survey.
777 Shen G., Lu Y., Zhou Q., Hong J., 2005. Interaction of polycyclic aromatic hydrocarbons and
778 heavy metals on soil enzyme. Chemosphere; 61: 1175-1182.
779 Singh J.P., Ojinnaka E.U., Krumins J.A., Goodey N.M., 2019a. Abiotic factors determine
780 functional outcomes of microbial inoculation of soils from a metal contaminated
781 brownfield. Ecotoxicol. Environ. Saf.; 168: 450-456.
782 Singh J.P., Vaidya B.P., Goodey N.M., Krumins J.A., 2019b. Soil microbial response to metal
783 contamination in a vegetated and urban brownfield. J. Environ. Manage.; 244: 313-319.
784 Smith M.J., Flowers T.H., Duncan H.J., Alder J., 2006. Effects of polycyclic aromatic
785 hydrocarbons on germination and subsequent growth of grasses and legumes in freshly
786 contaminated soil and soil with aged PAHs residues. Environ. Pollut.; 141: 519-525.
787 Speir T.W., Kettles H.A., Parshotam A., Searle P.L., Vlaar L.N.C., 1999. Simple kinetic
788 approach to determine the toxicity of AS[V] to soil biological properties. Soil Biol.
789 Biochem.; 31: 705-713.
790 Sprocati A.R., Alisi C., Tasso F., Marconi P., Sciullo A., Pinto V., et al., 2012. Effectiveness of a
791 microbial formula, as a bioaugmentation agent, tailored for bioremediation of diesel oil
792 and heavy metal co-contaminated soil. Process Biochem.; 47: 1649-1655.
793 Stout S.A., Emsbo-Mattingly S.D., 2008. Concentration and character of PAHs and other
794 hydrocarbons in coals of varying rank – Implications for environmental studies of soils
795 and sediments containing particulate coal. Org. Geochem.; 39: 801-819.
796 Suárez-Ruiz I., Flores D., Mendonça Filho J.G., Hackley P.C., 2012. Review and update of the
797 applications of organic petrology: Part 1, geological applications. Int. J. Coal Geol.; 99:
798 54-112.
799 Taylor G.H., Teichmüller M., Davis A., Diessel C., Littke R., Robert P., 1998 Organic petrology.
800 Gebrüder Borntraeger, Berlin.
801 Thornton I., Farago M.E., Thums C.R., Parrish R.R., McGill R.A.R., Breward N., et al., 2008.
802 Urban geochemistry: research strategies to assist risk assessment and remediation of
803 brownfield sites in urban areas. Environ. Geochem. and Health; 30: 565-576.
804 Tinoco P., Almendros G., Sanz J., González-Vázquez R., González-Vila F.J., 2006. Molecular
805 descriptors of the effect of fire on soils under pine forest in two continental
806 Mediterranean soils. Org. Geochem.; 37: 1995-2018.
807 Wang Z., Fingas M.F., 2003. Development of oil hydrocarbon fingerprinting and identification
808 techniques. Mar. Pollut. Bull.; 47: 423-452.
809 Wang Z., Stout S., 2010 Oil spill environmental forensics: fingerprinting and source
810 identification: Elsevier.

811 Wang Z., Yang C., Fingas M., Hollebone B., Peng X., Hansen A.B., et al., 2005.
812 Characterization, Weathering, and Application of Sesquiterpanes to Source Identification
813 of Spilled Lighter Petroleum Products. Environ. Sci. Technol.; 39: 8700-8707.
814 Wang Z., Yang C., Kelly-Hooper F., Hollebone B.P., Peng X., Brown C.E., et al., 2009. Forensic
815 differentiation of biogenic organic compounds from petroleum hydrocarbons in biogenic
816 and petrogenic compounds cross-contaminated soils and sediments. J. Chromatogr. A;
817 1216: 1174-1191.
818 Wiłkomirski B., Sudnik-Wójcikowska B., Galera H., Wierzbicka M., Malawska M., 2011.
819 Railway transportation as a serious source of organic and inorganic pollution. Water Air
820 Soil Pollut.; 218: 333-345.
821 Yunker M.B., Macdonald R.W., Veltkamp D.J., Cretney W.J., 1995. Terrestrial and marine
822 biomarkers in a seasonally ice-covered Arctic estuary — integration of multivariate and
823 biomarker approaches. Mar. Chem.; 49: 1-50.
824

Supplementary Figures

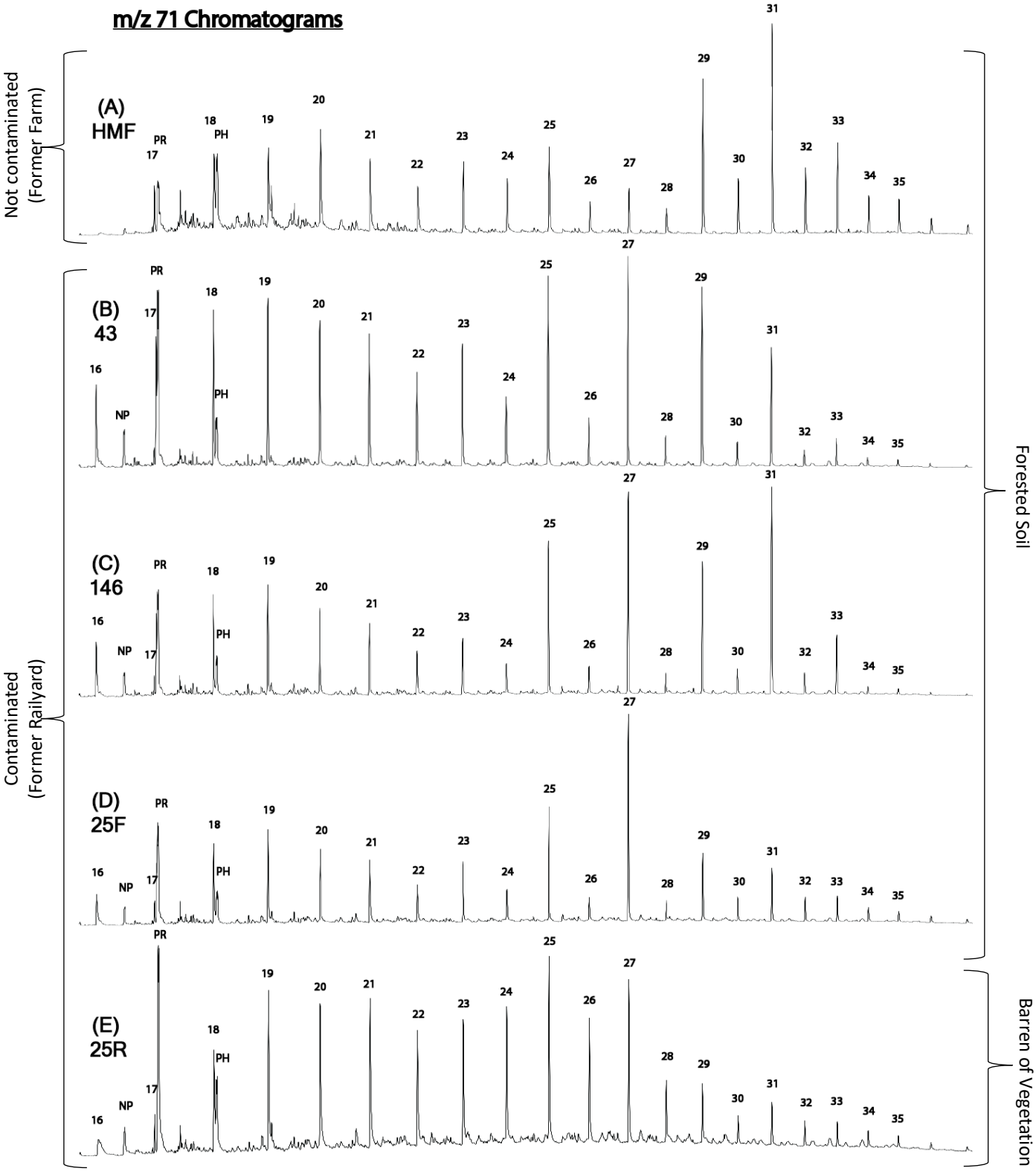


Fig. S1. Mass chromatograph (m/z 71) for all five samples (HMF, 146, 43, 25F, 25R), showing extracted normal alkanes with some isoprenoid compounds. See Table 1 for compound symbols.

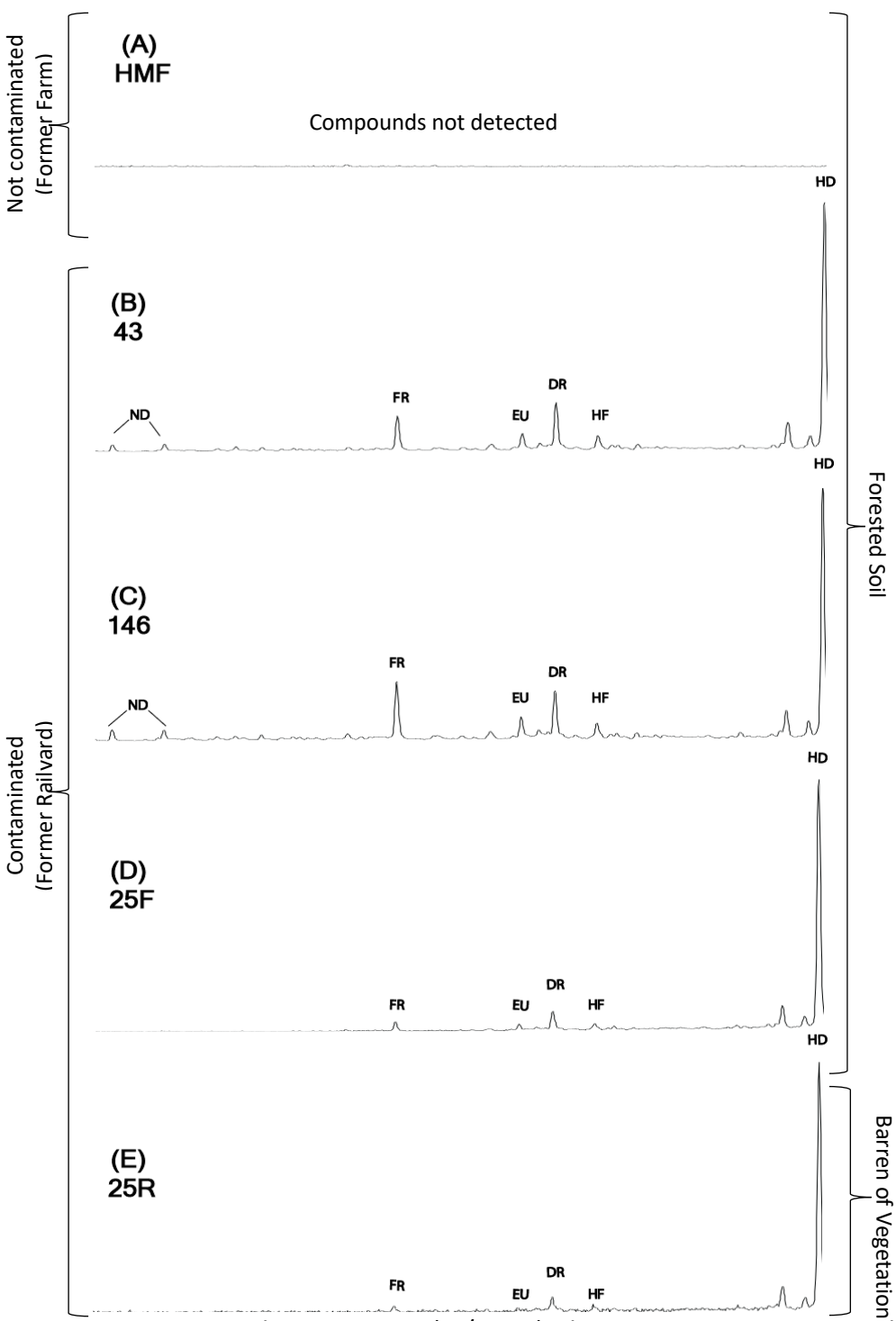


Fig. S2. Mass chromatogram (m/z 123), showing sesquiterpanes in all sample sites (HMF, 146, 43, 25F, and 25R); an indication of fossilized higher plant biomass. They are bicyclic compounds and the building components for triterpenoids. The compound symbols are as follows: nor-drimane (ND), farnesane (FR), 4A(H)-eudesmane (EU), 8B(H)-drimane (DR), homofarnesane (HF), 8B(H)-homodrimane (HD). Sesquiterpanes were not detected in HMF.

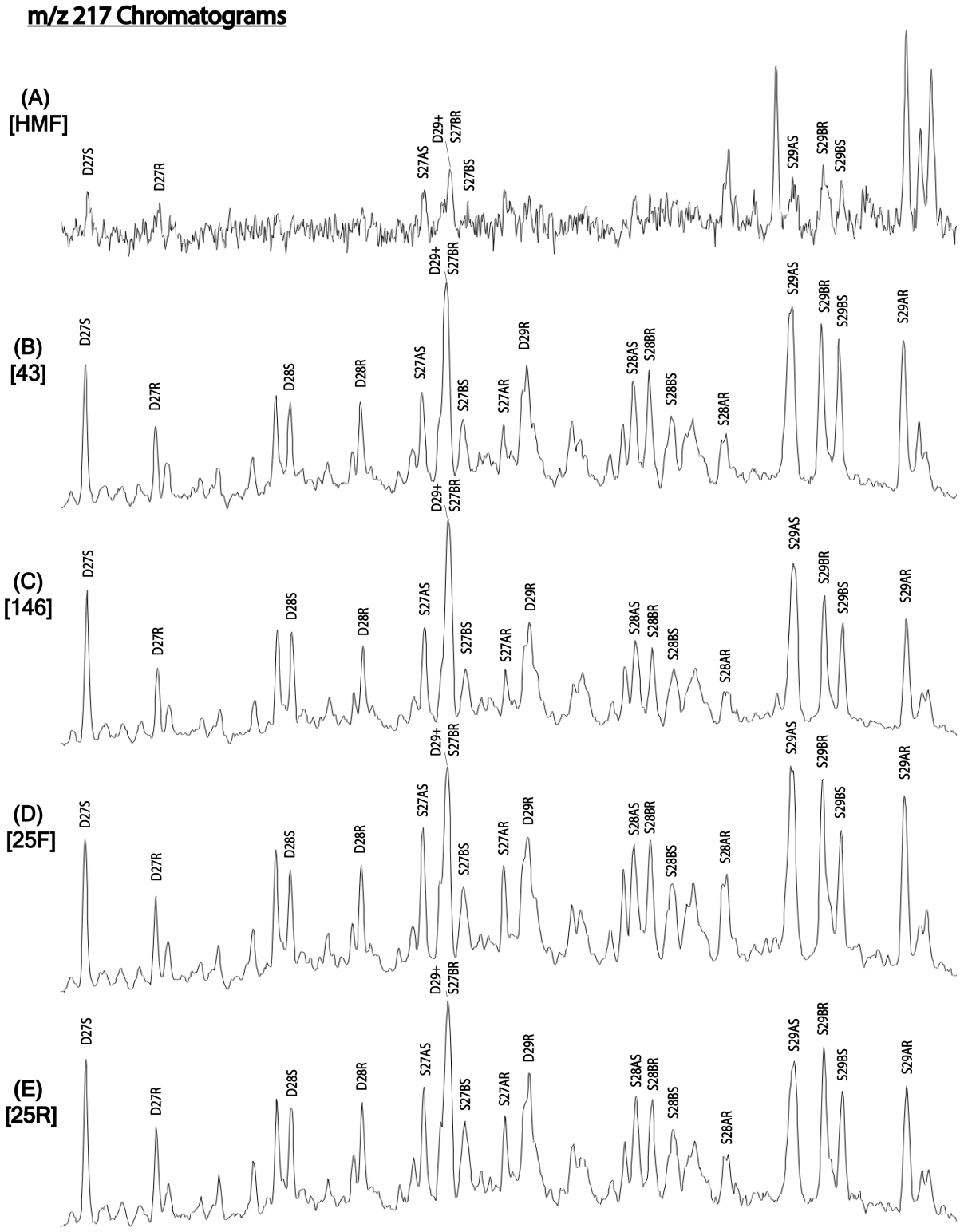


Fig. S3. Mass chromatogram (m/z 217), showing steranes in all sample sites (HMF, 146, 43, 25F, and 25R). The compound symbols are as follows:.

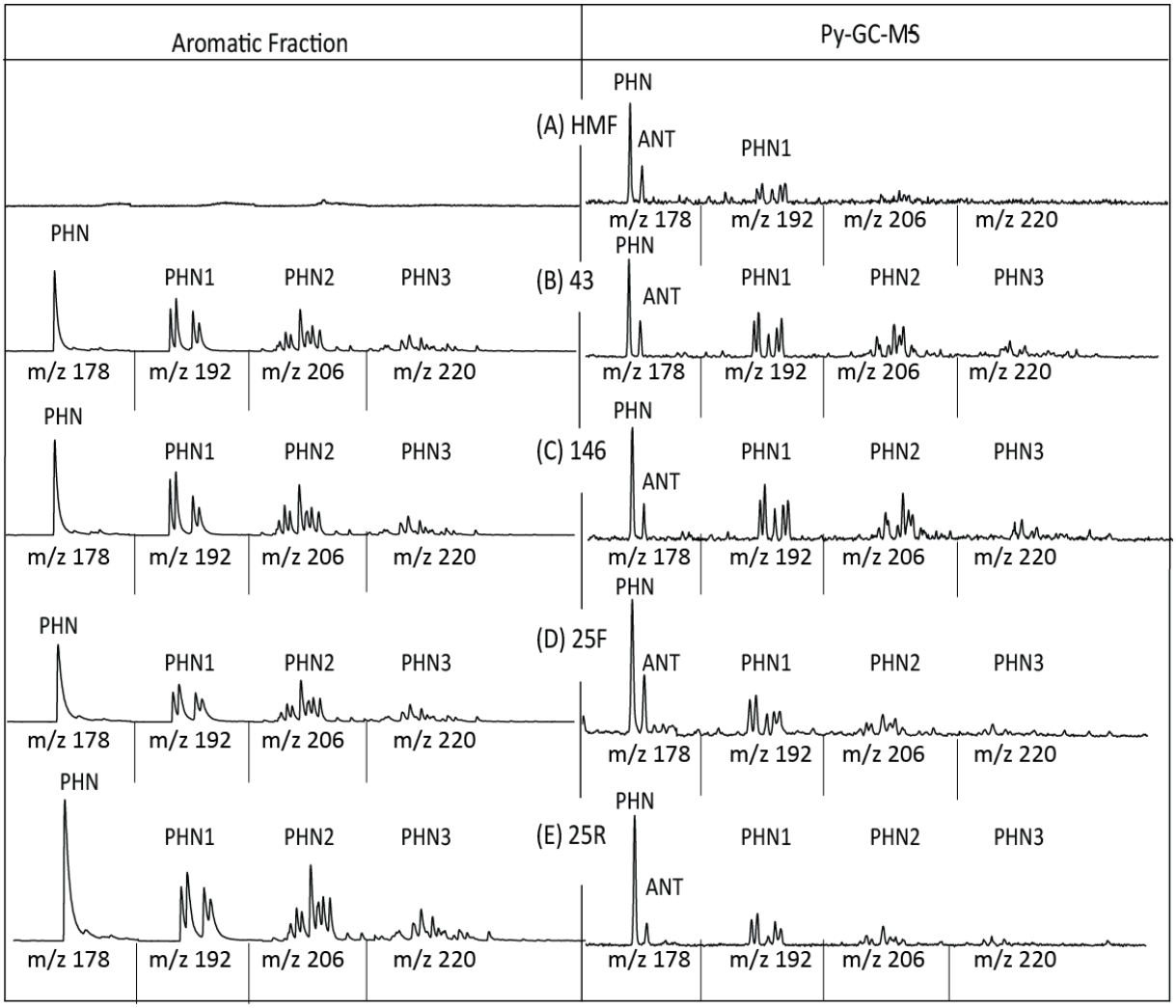


Fig. S4. Mass chromatograms (m/z 178, 192, 206, 220) showing the distribution of phenanthrene and methylated phenanthrenes in the aromatic fractions (on left) and Py-GC-MS (on right) of soil samples from HMF and LSP sites 43, 146, 25F and 25R. See Table 1 for compound symbols.

	43	146	25F	25R	HMF	Urban NJ Piedmont
mg/kg	Average ± standard error	Average ± standard error	Average ± standard error	Average ± standard error	Average ± standard error	Median
Li	7.7 ± 0.8	5.4 ± 0.7	24.1 ± 4.07	40.7 ± 12.4	23.8 ± 0.6	
Na	99 ± 8	218 ± 12	873 ± 129	4393 ± 669	47 ± 3	90.1
Mg	1240 ± 129	1477 ± 106	3132 ± 411	6213 ± 1819	3153 ± 60	2190
Al	4980 ± 325	5563± 1195	16132 ± 1519	20470 ± 4194	20527 ± 249	10500
P	429 ± 17	690 ± 14	684 ± 14	789 ± 49	534 ±48	
K	839 ± 80	686 ± 16	1737 ± 113	2697 ± 404	1927 ± 78	693
Ca	1948 ± 164	4065 ± 775	8228 ± 1402	10068 ± 1685	1542 ± 107	1425
Sc	2.06 ± 0.13	2.82 ± 0.25	2.40 ± 0.24	3.43 ± 0.48	3.06 ± 0.02	
V	32.9 ± 0.9	164 ± 8.3	70.7 ± 9.5	77.3 ± 11.8	30.1 ± 0.1	29.6
Cr	24.8 ± 0.7	118.0 ± 2.1	79.2 ± 3.2	165.2 ± 21.7	21.0 ± 0.3	18.5
Mn	159 ± 10	127 ± 4	460 ± 32	1042 ± 141	674 ± 56	311
Fe	34061± 1819	17520 ± 1491	179062 ± 22211	266653 ± 59863	18722 ± 1540	14600
Co	5.5 ± 0.4	6.2 ± 0.3	256.5 ± 46.5	868.7 ± 178.8	6.0 ± 0.1	6.3
Ni	21.1 ± 1.4	46.7 ± 0.9	121.4 ± 13.8	317.4 ± 62.5	18.5 ± 0.3	12.4
Cu	79 ± 4	93 ± 3	2256 ± 320	7165 ± 1512	18 ± 2	29.5
Zn	89 ± 4	180 ± 24	14435 ± 2845	41271 ± 8526	78 ± 4	75.3
As	17.8 ± 1.0	37.4 ± 4.5	630 ± 187	1162 ± 207	5.3 ± 0.1	5.2
Mo	3.5 ± 0.1	4.7 ± 0.4	29.3 ± 1.6	63.1 ± 10.1	1.6 ± 0.1	
Ag	0.42 ± 0.02	0.97 ± 0.01	3.80 ± 0.07	7.04 ± 0.79	0.58 ± 0.01	< D.L.
Cd	0.20 ± 0.01	0.63 ± 0.06	3.88 ± 0.63	7.74 ±	0.30 ± 0.02	< D.L.
Ba	88 ± 3	181 ± 15	533 ± 53	1467 ± 267	139 ± 4	80.6
Pb	215 ± 9	355 ± 18	7145 ± 1351	20302 ± 4203	28 ± 1	111

Supplement Table S1. Concentrations (μg/g) of elements listed in order of atomic weight for the average of HMF, 43, 146, 25F and 25R of three replicates. (1 ± S.E.). Urban NJ Piedmont is from Sanders 2003, where values indicated are the median concentration (mg/kg). < D.L. is below detection limit, which is Ag = 0.2 and Cd = 0.4 mg/kg.